Lithos xxx (2014) xxx–xxx

Contents lists available at ScienceDirect

Lithos

journal homepage: www.elsevier.com/locate/lithos

Prograde and retrograde evolution of eclogite from Adrar Izzilatène (Egéré-Aleksod terrane, Hoggar, Algeria) determined from chemical zoning and pseudosections, with geodynamic implications

Sid Ali Doukkari [a,*], Khadidja Ouzegane [a], Gaston Godard [b], Johann F.A. Diener [c], Jean-Robert Kienast [b], Jean-Paul Liégeois [d], Amar Arab [a], Amar Drareni [a]

[a] Laboratoire de Géodynamique, Géologie de l'Ingénieur et de Planétologie, FSTGAT-U.S.T.H.B., B.P. 32 El Alia, Dar el Beida, Alger 16111, Algeria
[b] Institut de Physique du Globe de Paris, Sorbonne Paris Cité, Université Paris-Diderot, UMR 7154 CNRS, 1 rue Jussieu, Paris 75238, France
[c] Department of Geological Sciences, University of Cape Town, Private Bag X3, Rondebosch 7701, South Africa
[d] Geodynamics and Mineral Resources, Royal Museum for Central Africa, Tervuren B-3080, Belgium

ARTICLE INFO

Article history:
Received 28 May 2014
Accepted 13 December 2014
Available online xxxx

Keywords:
Prograde eclogite
Hoggar
Chemical zoning
P–T pseudosection

ABSTRACT

Adrar Izzilatène in the Egéré-Aleksod terrane of the LATEA metacraton (Hoggar, Algeria) exposes one of the best preserved examples of eclogite facies metamorphism in Hoggar. Three distinct stages of metamorphic development are recognised, namely, the pre-peak stage (M1), characterised by garnet, amphibole, epidote, quartz and rutile, the peak eclogite facies stage (M2), consisting of omphacite, garnet, edenite, epidote, quartz and rutile, and the retrograde stage (M3), where initial decompression resulted in the appearance of plagioclase, the development of pargasite + plagioclase kelyphites and finally the formation of anhydrous plagioclase + diopside coronas. Porphyroblastic omphacite has a jadeite content of up to $X_{Jd} = 0.36$, which is the highest yet observed for eclogite facies rocks from the Tuareg Shield. Garnet growth zoning patterns are characterised by flat profiles in the cores ($X_{Alm} = 0.55–0.60$; $X_{Prp} = 0.12–0.16$; $X_{Grs} = 0.26–0.30$) before showing a decrease in almandine to $X_{Alm} = 0.45$, coupled to an increase in pyrope to $X_{Prp} = 0.29$ and decrease in grossular to $X_{Grs} = 0.26$ at the rims. Calculated $P–T–M_{H2O}$ pseudosections show that the prograde M1 assemblage equilibrated at 13–14 kbar and 580 °C, before pressure and temperature increased to 19 kbar and 650–700 °C at fluid-saturated conditions during peak metamorphism. Retrogression involved near-isothermal decompression to 8–9 kbar and 700–750 °C at fluid-undersaturated conditions. Prograde-to-peak metamorphism of the Izzilatène eclogite could have involved either oceanic or continental subduction, followed by exhumation as the area was obducted towards the LATEA metacraton during the Pan-African orogeny and the assembly of Western Gondwana.

1. Introduction

The Tuareg Shield represents a part of the Trans-Saharan Pan-African orogenic belt and is composed of 23 displaced terranes that are separated by subvertical strike-slip shear zones or major thrust fronts (e.g., Cahen et al., 1984; Black et al., 1994; Fig. 1a). These terranes, amalgamated together during the Pan-African orogenic cycle between 870 and 540 Ma, have different origins and are composed of either variably reworked Archaean to Paleoproterozoic domains (referred to as metacratons by Liégeois et al., 2013), or of juvenile Neoproterozoic units (Caby, 2003; Fezaa et al., 2010; Liégeois et al., 2003; Ouzegane et al., 2003; Peucat et al., 2003 and references therein). These terranes are further characterised by a marked absence of Mesoproterozoic rocks or events (e.g., Fezaa et al., 2010; Peucat et al., 2003). The Pan-African orogeny is related to the formation of the Gondwana supercontinent, and in the Tuareg Shield, this involved the accretion of several island arcs before the final collisional stage at 630–580 Ma. During final collision, the Shield was involved in northwards-directed tectonic escape as it was being squeezed between the West African craton and the Saharan metacraton (Black et al., 1994; Dostal et al., 2002; Liégeois et al., 2003, 2013).

The Tuareg Shield is known for the occurrence of Precambrian rocks that experienced high-pressure eclogite facies metamorphism during the accretionary stage of the Pan-African orogeny (Berger et al., 2014; Bertrand, 1974; Derridj et al., 2010; Doukkari et al., 2014; Liégeois et al., 2003; Sautter, 1985; Zetoutou et al., 2004). These eclogite facies rocks have principally been described in the Central Hoggar (Southern Algeria), but have recently also been discovered in Western Hoggar (Berger et al., 2014). The preservation of the pre-collisional eclogite metamorphic imprint occurred through the obduction of these rocks onto a rigid continental terrane, thereby shielding them from later collisional processes (Liégeois et al., 2003). The subsequent Phanerozoic geological evolution of Hoggar is limited to Cenozoic intraplate volcanism (Liégeois et al., 2005 and references therein) and doming-related

* Corresponding author.
E-mail address: sidali.doukkari@gmail.com (S.A. Doukkari).

http://dx.doi.org/10.1016/j.lithos.2014.12.007
0024-4937/

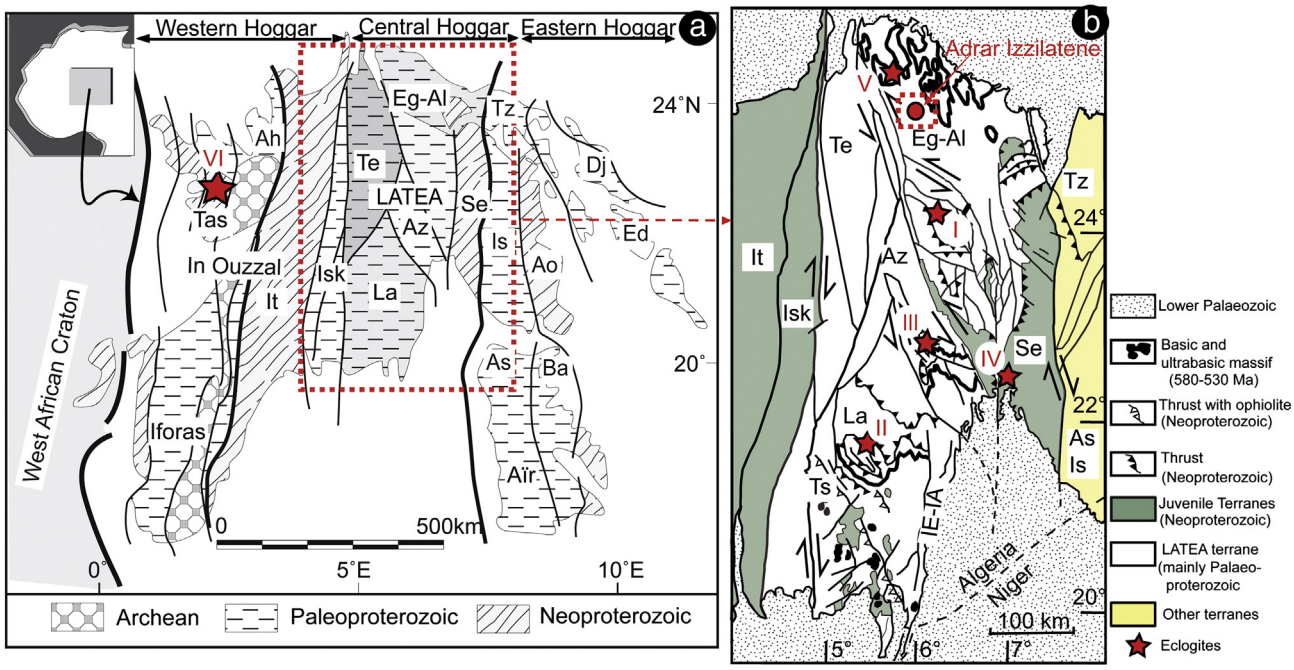

Fig. 1. (a) Schematic map of the various terranes that constitute the Tuareg Shield, highlighting the location of the LATEA metacraton in the boxed outline(after Caby, 2003). (b) Sketch map of the internal architecture of the LATEA metacraton after Liégeois et al. (2003), with the location of the Adrar Izzilatène eclogite indicated by the boxed outline. The stars show the location of eclogites in LATEA: (I) Aleksod, (II) Tin Begane, (III) Azrou N'Fad, (IV) Serouenout, (V) Tighsi, (VI) Tassendjanet (in a). Ah = Ahnet; Ao = Aouzegueur; As = Assode; Ba = Barghot; Ed = Edembo; Djanet; Is = Issalane; Tas = Tassendjanet; Se = Serouenout; Eg-Al = Egéré-Aleksod; Te = Tefedest; Az = Azrou-N-Fad; La = Laouni; Isk = Iskel; It = In Teidini; Tz = Tazat.

uplift during the Eocene (Rougier et al., 2013). Consequently, the eclogites have not been reworked by later tectonic events and are relatively pristine, such that their entire metamorphic history has potentially been preserved. This offers the rare opportunity for the prograde history of eclogites to be investigated because whereas the peak-to-retrograde history of eclogites is typically well constrained from reaction textures that replace garnet and omphacite during retrogression (e.g., Carson et al., 1999; Cruciani et al., 2012; Fitzherbert et al., 2005; Godard, 2001), the prograde evolution is usually much more cryptic, having to be gleaned from mineral inclusions or chemical zoning (e.g., Berger et al., 2014; Groppo et al., 2009; Štípská and Powell, 2005).

This study investigates eclogites collected at Adrar Izzilatène in the Egéré-Aleksod terrane of Central Hoggar, South Algeria, and provides detailed petrological, textural and mineralogical data from which the metamorphic history of the rocks is determined. Key evidence for the prograde path comes from preserved mineral compositional zoning and inclusions. Calculated pseudosections and compositional isopleths are used to quantify the prograde as well as the retrograde parts of the *P–T* path. In turn, this evolution allows the early Pan-African events that occurred in Central Hoggar to be constrained, thereby shedding new light on the amalgamation of the Tuareg Shield, and by extension, the formation of Western Gondwana.

2. Geological setting and previous work

Traditionally, the Tuareg Shield has been subdivided into three parts, with the western part being mostly juvenile and Neoproterozoic in age, the eastern part being of more enigmatic origin and possibly related to an eastern craton, and the central part being dominated by old metamorphic lithologies that are intruded by granitoids (e.g., Bertrand and Caby, 1978). More recent investigations have confirmed that the western part of the Shield appears to predominantly be related to the closure of the ocean that separated the Tuareg Shield from the West African craton (Berger et al., 2011, 2014; Caby, 2003; Caby and Andréopoulos-Renaud, 1987; Caby and Monié, 2003; Caby et al., 1989; Dostal et al., 1994; Liégeois et al., 1987), although it also contains older, inherited material such as the In Ouzzal terrane (Caby, 1996; Ouzegane et al., 2003). The eastern part appears to be a part of the Saharan metacraton that has been pervasively reworked until ca. 540 Ma (Fezaa et al., 2010; Nouar et al., 2011). By contrast, Central Hoggar is characterised by the presence of well-preserved Archaean and Paleoproterozoic lithologies, high-pressure eclogite-bearing nappes and abundant 630–580 Ma granitoid plutons and batholiths (Abdallah et al., 2007; Barbey et al., 1989; Bendaoud et al., 2004, 2008; Bertrand et al., 1986; Doukkari et al., 2014; Liégeois et al., 2003; Peucat et al., 2003; Sautter, 1985, 1986; Zetoutou et al., 2004). The absence of lithological associations characteristic of active margins has led to the proposal that the Central Hoggar was a passive margin during the Neoproterozoic, before it was first partially subducted during the convergent stage of the Pan-African orogeny and then laterally extruded during the collisional phase (Liégeois et al., 2003). As a consequence, Central Hoggar is dissected by strike-slip shear zones that separate displaced terranes (Black et al., 1994). These shear zones were later intruded by granitoid batholiths (Acef et al., 2003; Liégeois et al., 2003) and also form areas of localised reworking of Eburnian and Pan-African high-pressure lithologies (Bendaoud et al., 2008). However, areas away from the shear zones have remained intact since their assembly, indicating that Central Hoggar exhibits the characteristics of a metacraton (Liégeois et al., 2013). This metacraton has been termed LATEA, the acronym of its constituting displaced terranes (Laouni, Azrou n'Fad, Tefedest, Egéré-Aleksod; Liégeois et al., 2003; Fig. 1b).

The basement of the various terranes that constitute the LATEA metacraton vary from Archaean (~2.7 Ga) to Paleoproterozoic (2.1–1.9 Ga) in age and have been metamorphosed to amphibolite or granulite facies conditions (Barbey et al., 1989; Bendaoud et al., 2008; Bertrand et al., 1986; Peucat et al., 2003). The high-pressure lithologies found in the LATEA metacraton occur either as old basement lenses that have been transformed within Pan-African shear zones (Sautter, 1985, 1986), or as allochthonous juvenile Neoproterozoic sheets (Liégeois et al., 2003). An example of the latter occurrence is the Tin Begane area, where rocks exhibit positive ε_{Nd} values, low Sr initial ratios, Neoproterozoic Nd T_{DM} model ages and Sm-Nd mineral isochron ages of 685 ± 19 Ma (Liégeois et al., 2003). In other parts of the world, eclogite facies rocks derived from such different protoliths have been interpreted

Please cite this article as: Doukkari, S.A., et al., Prograde and retrograde evolution of eclogite from Adrar Izzilatène (Egéré-Aleksod terrane, Hoggar, Algeria) determined from chemical..., Lithos (2014), http://dx.doi.org/10.1016/j.lithos.2014.12.007

to indicate subduction of a passive margin (e.g., the Western Gneiss Region of the Baltic Shield; Hacker et al., 2010; Maupin et al., 2013).

2.1. Previous metamorphic investigations of eclogites in Hoggar

Eclogite facies assemblages in the Aleksod unit (Fig. 1b, locality I) were first described by Bertrand (1974), and later recognised in metabasic lenses by Sautter (1985), who estimated their *P–T* conditions at 750 °C and > 15 kbar. In the Tin Begane area of the Laouni terrane (Fig. 1b, locality II), retrograde *P–T–t* paths are proposed to have involved decompression-heating from peak eclogite facies conditions of more than 15 kbar and ~790 °C to garnet amphibolite conditions of 12 kbar and 830 °C at 685 ± 19 Ma (Liégeois et al., 2003). In the Azrou N'Fad terrane (Fig. 1b, locality III), these rocks are only preserved in the core of isolated lenses whose margins have been pervasively amphibolitised (Zetoutou et al., 2004). A metamorphic peak is calculated at approximately 760 ± 50 °C and at minimum pressure of 15 ± 1.5 kbar, with near-isothermal decompression leading to retrograde conditions of 700–750 °C and 11 ± 1.6 kbar (Zetoutou et al., 2004). In the south of the Serouenout terrane (Fig. 1b, locality IV), granulitised eclogite rocks are associated with talc-kyanite whiteschists (Adjerid et al., 2012, in this volume; Derridj et al., 2010). Here, the peak omphacite (Jd_{30})–garnet paragenesis constrains eclogite facies conditions of 17 kbar and 650 ± 50 °C, with the granulite facies overprint producing orthopyroxene-plagioclase symplectites at conditions of 10 kbar and 813 ± 60 °C (Adjerid et al., 2012; Derridj et al., 2010).

Whereas the metamorphic evolution of the Hoggar eclogite facies rocks has been described in general terms, much of the details of their evolution, and particularly the characteristics of the prograde path, have not been determined. One reason for this is that all of the *P–T* estimates cited above were determined by conventional geothermobarometry, and these rocks have not been investigated with petrological modelling techniques capable of producing more complete *P–T* paths (e.g., Berger et al., 2014; Groppo et al., 2009; Štípská and Powell, 2005). So far, the only investigation on these rocks using modern petrological modelling techniques concerns eclogite from the Tighsi area in the northern part of the Egéré-Aleksod terrane (Fig. 1b, locality V; Doukkari et al., 2014) and eclogite and garnetiferous amphibolite from the Tassendjanet terrane in Western Hoggar (Fig. 1a, locality VI; Berger et al., 2014).

In the Tighsi area, eclogite and the garnet amphibolite occur as lenses in marble, metapelite and quartzite. The high-pressure paragenesis (omphacite–garnet–rutile–quartz and epidote, with epidote, rutile and quartz inclusions in omphacite; Doukkari et al., 2014) was destabilised during decompression, giving rise to very thin symplectites of albite and jadeite-poor clinopyroxene, as well as kelyphites and amphibole–plagioclase symplectites separating garnet from omphacite and quartz (Doukkari et al., 2014). The *P–T* conditions of the high-pressure stage are estimated at 19.5 kbar and 700 °C, with retrogression estimated to have involved near-isothermal decompression to 9.3 kbar and 700 °C (Doukkari et al., 2014). In the Tassendjanet terrane, thermodynamic modelling has constrained a high-pressure clockwise *P–T* path, with peak eclogite conditions of 20–22 kbar and 650 °C followed by exhumation and minor heating to 10–14 kbar at 730 °C, before the rocks cooled to conditions of 7–10 kbar and 610 °C (Berger et al., 2014).

2.2. Geology of Adrar Izzilatène

The studied locality at Adrar Izzilatène occurs in the central part of the Egéré area and is located along the northwestern boundary of the Egéré-Aleksod terrane (Fig. 1b). This locality exposes one of the best preserved examples of eclogite facies metamorphism in Hoggar.

The first description of the Egéré Precambrian basement was provided by Lelubre (1952). He distinguished two metamorphic series: an older one consisting of migmatitic orthogneisses (Arechchoum gneisses), and a metasedimentary cover sequence containing numerous interlayered garnet amphibolite lenses (Egéré series). The area was remapped in detail by Duplan (1972), who recognised intense folding and strong flattening in the Egéré series. Occurrences of eclogite in the Egéré-Aleksod terrane were interpreted by Latouche (1985) as exotic tectonic units, underlying a megathrust separating them from the adjacent, apparently lower-grade, metasedimentary rocks. However, recent work has shown that high-pressure mineral assemblages are also found in marbles and metapelites associated with eclogite (Arab et al., 2014), indicating that the eclogitic rocks are not exotic to the metasedimentary sequence. Significantly, no trace of eclogite facies metamorphism is found in the migmatitic orthogneisses of the Arechchoum series. It is thus likely that the contact between the Arechchoum and Egéré series is tectonic, with the two series potentially differing by their origin and nature and having a different geochronology and metamorphic evolution.

Field occurrences of eclogite at Adrar Izzilatène consist of well-preserved mafic eclogite lenses of 1 metre to several tens of metres in length, occurring within metasedimentary rocks dominated by eclogite facies marbles with subordinate Fe-rich quartzite and kyanite-garnet metapelites (Fig. 2a,b). Mafic eclogite lenses are more competent than the enveloping marbles and have a coarse-grained and massive texture compared to the mylonitic fabrics exhibited by the marbles. Because most of the deformation was partitioned into the marbles, the eclogites preserve their primary assemblages with only minor and localised retrograde overprints.

3. Petrography

The mineral inclusions and reaction textures of two eclogite samples (Eg18; 25°49′22″N, 06°06′55″E and Eg82; 25°48′29″N, 06°06′56″E) were investigated using SEM imaging at the University of Paris VI. Both samples consist of coarse garnet, omphacite and amphibole grains

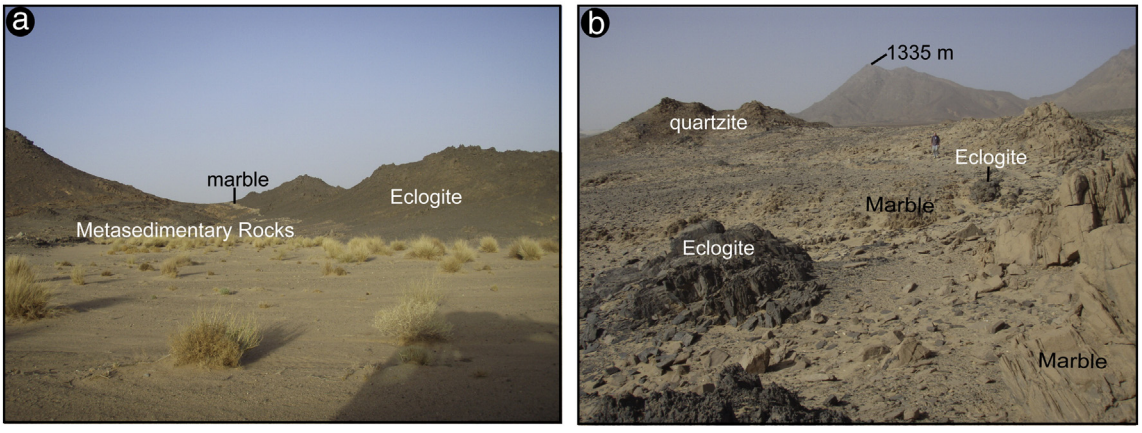

Fig. 2. Outcrop photographs of the Egéréeclogites. (a) Large eclogitelens associated with marble. (b) Metre-scale eclogite boudins hosted in marble.

Please cite this article as: Doukkari, S.A., et al., Prograde and retrograde evolution of eclogite from Adrar Izzilatène (Egéré-Aleksod terrane, Hoggar, Algeria) determined from chemical..., Lithos (2014), http://dx.doi.org/10.1016/j.lithos.2014.12.007

that are pervasively replaced by fine-grained symplectic assemblages of diopsidic clinopyroxene, amphibole and plagioclase (Fig. 3). Minor quartz occurs as recrystallised aggregates and epidote, rutile and ilmenite are present as accessory phases. The coarse-grained garnet–omphacite–amphibole assemblage is interpreted to reflect the prograde to peak metamorphic stages, whereas the symplectic diopsidic clinopyroxene–plagioclase assemblage and amphibole corona are interpreted to have formed during the post-peak, retrograde evolution, and inclusions within the porphyroblasts are interpreted to have been trapped under prograde conditions.

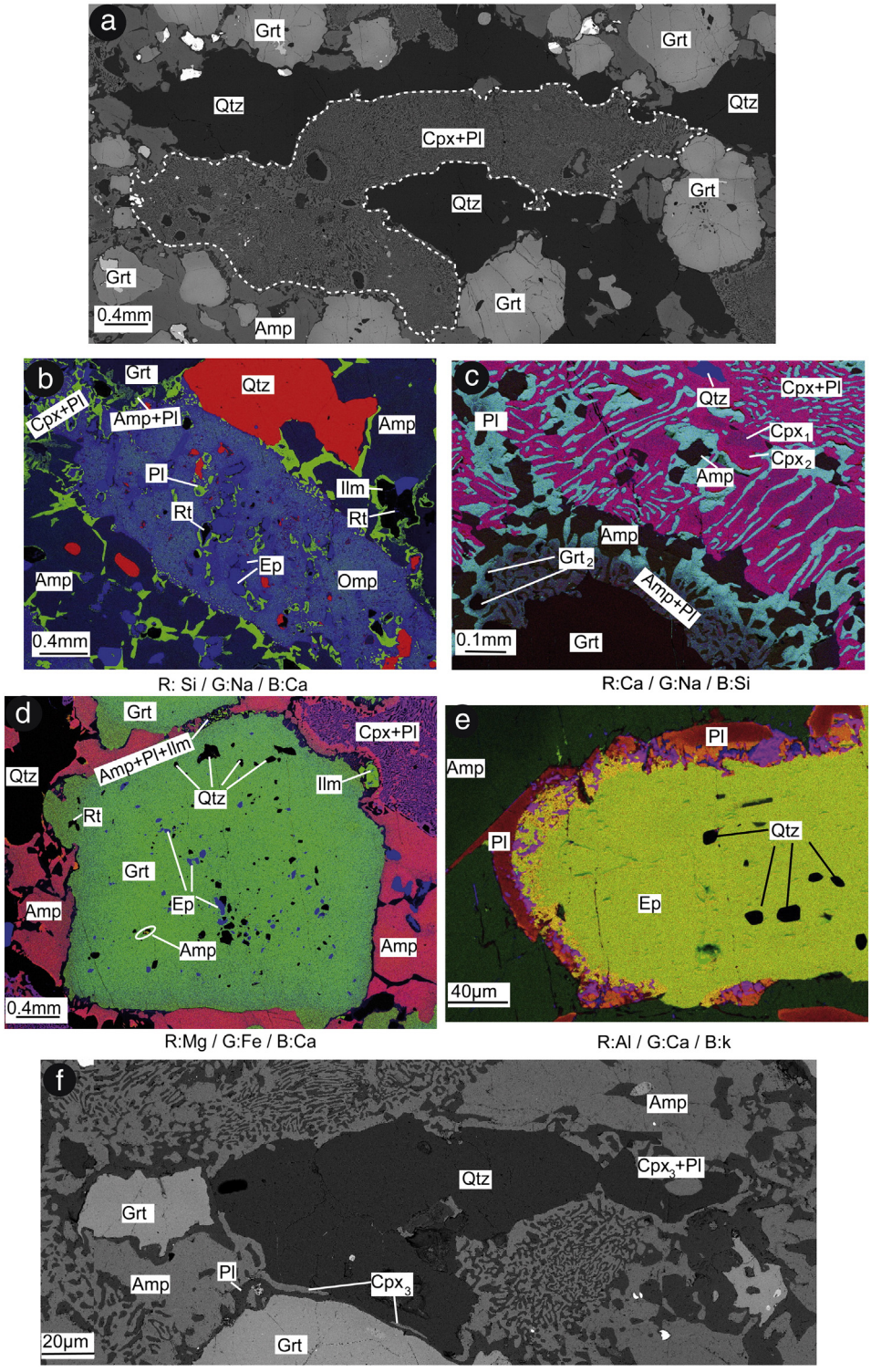

Fig. 3. BSE and RGB (R: red, G: green, B: blue) backscattered SEM images showing the general textures in sample Eg18. (a) Coarse-grained crystals of garnet, amphibole and quartz associated with very fine-grained clinopyroxene + plagioclase symplectites that pseudomorph original omphacite. (b) Preserved omphacite with epidote and quartz inclusions. (c) Corona and symplectite developed between garnet and omphacite, reflecting the model reaction$Grt_1 + Cpx_1 + H_2O \rightarrow Amp + Cpx_2 + Pl + Grt_2$. (c) Inclusions of epidote, quartz, amphibole and rutile in garnet. (d) Epidote with quartz inclusions, showing a corona of zoned plagioclase where it is in contact with amphibole. (e) Corona and symplectite of Cpx_3 and plagioclase developed at the boundary between amphibole-quartz and garnet-quartz. All mineral abbreviations after Kretz (1983): Grt, garnet; Qz, quartz; Amp, amphibole; Pl, plagioclase; Cpx, clinopyroxene; Rt, rutile; Ilm, ilmenite; Ep, epidote. (For interpretation of the references to colour in this figure, the reader is referred to the web version of this article.)

Please cite this article as: Doukkari, S.A., et al., Prograde and retrograde evolution of eclogite from Adrar Izzilatène (Egéré-Aleksod terrane, Hoggar, Algeria) determined from chemical..., Lithos (2014), http://dx.doi.org/10.1016/j.lithos.2014.12.007

Omphacite is light green in plane-polarised light and occurs as coarse-grained, 2 to 3.5 mm-sized porphyroblasts that often contain inclusions of epidote (Fig. 3b). Omphacite is partially to pervasively replaced by more diopsidic clinopyroxene–plagioclase symplectites; however, the symplectites typically pseudomorph the shape of the original omphacite grain (Fig. 3a). Two texturally distinct types of garnets are observed. The first most common garnet generation occurs as 1.5 to 4 mm-sized subhedral porphyroblasts that are pervasively rimmed by amphibole–plagioclase (kelyphite) symplectites (Fig. 3c). The second garnet type is much rarer and only occurs as fine-grained, 20 to 40 μm crystals in the kelyphite micro-domains (Grt2 in Fig. 3c). A notable feature of the coarse–grained garnet is the ubiquitous presence of epidote, quartz, amphibole and rutile inclusions that are concentrated in the cores of the crystals (Fig. 3d). Quartz and epidote inclusions are volumetrically more abundant than rutile and amphibole.

Two to 3 mm-sized amphibole porphyroblasts, locally show petrographic zoning with blue-green cores overgrown by brown-green rims. However, more frequently, amphibole in the matrix displays no discernible petrographic zoning, except where it becomes brown when in contact with ilmenite. Amphibole porphyroblasts are partly surrounded and replaced by plagioclase and clinopyroxene coronas where they are in contact with quartz or garnet (Fig. 3f). Small epidote grains occur as inclusions in garnet and omphacite (Fig. 3b, d) and also in the matrix of the sample. Matrix epidote is often surrounded by a fine corona of plagioclase (Fig. 3e). Rutile is present as inclusions in garnet as well as an accessory phase in the matrix of the samples, where it is associated with minor ilmenite (Fig. 3b).

4. Mineral composition and zoning

The chemical composition of the phases was determined using a Cameca SX100 electron microprobe at the University of Paris VI with operating conditions of 15 kV and 10 nA. Analyses were quantified using natural mineral standards and representative analyses of minerals are represented in Tables 1, 2, 3 and 4.

4.1. Garnet

Garnet is almandine-rich, with X_{Alm} varying between 0.46 and 0.60 (Table 1). Three compositionally distinct zones can be recognised in garnets from sample Eg82, with zones defined by the cores, inner and outer rims of grains (Fig. 4a). Zoning is characterised by relatively flat profiles in the cores of the grains ($Alm_{0.50–0.56}$ $Prp_{0.17–0.20}$ $Grs_{0.23–0.26}$ $Sps_{0.05–0.01}$) before showing a decrease in X_{Fe} towards the inner rim ($Alm_{0.50}$ $Prp_{0.27}$ $Grs_{0.23}$ $Sps_{0.00}$; Fig. 4a). A sharp opposite trend is seen in the outer rim (up to $Alm_{0.60}$ $Prp_{0.20}$ $Grs_{0.20}$ $Sps_{0.00}$; Fig. 4a).

Garnet from sample Eg18 shows a similar core–inner rim zoning profile (Fig. 4b) but lacks the marked trend seen in the outer rim of garnet in Eg82 (see Fig. 4a). Zoning is characterised by relatively flat profiles in the cores ($Alm_{0.55–0.60}$ $Prp_{0.12–0.16}$ $Grs_{0.26–0.30}$ $Sps_{0.07–0.01}$), before showing an increase in pyrope, coupled to decreases in almandine and grossular, at the rims (up to $Alm_{0.45}$ $Prp_{0.29}$ $Grs_{0.26}$ $Sps_{0.00;}$ Fig. 4b). Compared to the rims of the coarse-grained garnet, the small garnets in the kelyphite of the same sample (Grt_2 in Fig. 3c) are richer in almandine and poorer in pyrope, but with comparable grossular content ($Alm_{0.54}$ $Prp_{0.20}$ $Grs_{0.24}$ $Sps_{0.00}$; Table 1).

4.2. Clinopyroxene

Omphacite porphyroblasts (Cpx_1) in sample Eg18 have a jadeite content of up to $X_{Jd} = 0.36$ (Table 2; Fig. 4c), which is the highest yet observed for eclogites from the Tuareg Shield. Omphacite shows a flat compositional profile (Fig. 4d) in the core but is marked by a sharp decrease in jadeite content at the rims ($X_{Jd} = 0.15$), which is manifested by a reverse jadeitic substitution, where Ca, Fe and Mg replace Na and Al^{VI} (Fig. 4e). Diopsidic clinopyroxene (Cpx_2) present in the Cpx_2 + plagioclase symplectites has variable, but much lower jadeite

Table 1
Representative electron microprobe data of garnet.

Sample	Eg18	Eg18	Eg18	Eg18	Eg18	Eg82	Eg82	Eg82	Eg82	Eg82
	core	core	core	rim	grt2	core	core	core	Inner rim	outer rim
SiO_2	37.56	38.21	37.26	38.56	37.63	38.45	38.62	38.48	38.91	39.32
TiO_2	0.08	0.07	0.08	0.08	0.04	0.73	0.09	0.05	0.06	0.06
Al_2O_3	20.98	21.40	20.85	21.15	21.01	20.85	22.00	21.67	22.00	22.68
Cr_2O_3	0.02	0.01	0.02	0.03	0.02	0.00	0.00	0.00	0.00	0.00
FeOt	27.61	25.85	24.87	23.03	25.36	23.66	24.51	23.58	23.21	24.76
MnO	1.37	0.60	0.10	0.15	0.41	0.99	1.10	0.15	0.23	0.37
MgO	3.20	3.74	3.92	6.73	5.26	6.27	4.97	5.53	6.36	5.08
NiO	0.00	0.00	0.00	0.00	0.00	0.00	0.00	0.00	0.00	0.00
CaO	8.59	10.07	11.11	9.09	8.48	7.97	8.47	10.42	9.49	7.52
Na_2O	0.03	0.00	0.00	0.02	0.03	0.06	0.06	0.04	0.05	0.06
K_2O	0.02	0.00	0.01	0.00	0.01	0.06	0.01	0.01	0.01	0.00
Total	99.47	99.97	98.20	98.83	98.24	99.05	99.82	99.94	100.33	99.85
Equ. O	12.00	12.00	12.00	12.00	12.00	12.00	12.00	12.00	12.00	12.00
Si	2.98	3.00	2.96	3.00	2.98	3.01	3.01	2.98	2.99	3.06
AlVI	1.97	1.97	1.96	1.94	1.96	1.92	2.02	1.97	1.99	2.08
Ti	0.00	0.00	0.00	0.00	0.00	0.04	0.01	0.00	0.00	0.00
Cr	0.00	0.00	0.00	0.00	0.00	0.00	0.00	0.00	0.00	0.00
Fe3 +	0.04	0.02	0.07	0.05	0.05	0.04	0.00	0.04	0.02	0.00
Fe2 +	1.79	1.68	1.58	1.45	1.63	1.51	1.60	1.48	1.47	1.61
Mg	0.38	0.44	0.46	0.78	0.62	0.73	0.58	0.64	0.73	0.59
Ni	0.00	0.00	0.00	0.00	0.00	0.00	0.00	0.00	0.00	0.00
Mn	0.09	0.04	0.01	0.01	0.03	0.07	0.07	0.01	0.02	0.02
Ca	0.73	0.85	0.95	0.76	0.72	0.67	0.71	0.86	0.78	0.63
Na	0.00	0.00	0.00	0.00	0.00	0.01	0.01	0.01	0.01	0.01
K	0.00	0.00	0.00	0.00	0.00	0.01	0.00	0.00	0.00	0.00
Total	8.00	8.00	8.00	8.00	8.00	8.00	8.00	8.00	8.00	8.00
XFe	0.83	0.79	0.77	0.65	0.72	0.67	0.73	0.70	0.67	0.73
Alm	0.60	0.56	0.53	0.48	0.54	0.51	0.54	0.50	0.49	0.57
Sps	0.03	0.01	0.00	0.00	0.01	0.02	0.02	0.00	0.01	0.01
Grs	0.24	0.28	0.32	0.25	0.24	0.22	0.24	0.29	0.26	0.22
Prp	0.13	0.15	0.15	0.26	0.21	0.25	0.20	0.21	0.24	0.21

Please cite this article as: Doukkari, S.A., et al., Prograde and retrograde evolution of eclogite from Adrar Izzilatène (Egéré-Aleksod terrane, Hoggar, Algeria) determined from chemical..., Lithos (2014), http://dx.doi.org/10.1016/j.lithos.2014.12.007

Table 2
Representative electron microprobe data of clinopyroxene.

Sample	Eg18	Eg18	Eg18	Eg18	Eg18	Eg18	Eg18	Eg82	Eg82	Eg82	Eg82
	Cpx1 core	Cpx1 core	Cpx1 rim	Cpx2	Cpx2	Cpx3	Cpx312*	Cpx1	Cpx1	Cpx2	Cpx2
SiO_2	53.66	56.53	52.10	53.70	53.09	50.65	53.35	53.45	52.34	51.79	53.12
Al_2O_3	8.64	8.63	6.40	7.53	2.20	3.22	9.38	9.38	9.20	8.53	1.39
TiO_2	0.16	0.15	0.13	0.22	0.06	0.03	0.10	0.11	0.16	0.18	0.07
Cr_2O_3	0.06	0.02	0.05	0.03	0.12	0.08	0.01	0.01	0.01	0.00	0.03
FeO	6.09	5.57	8.17	6.88	7.86	8.02	5.26	6.47	6.93	7.98	7.97
MnO	0.01	0.00	0.09	0.02	0.06	0.04	0.02	0.00	0.00	0.09	0.08
MgO	9.78	9.35	11.09	11.23	13.67	14.61	8.79	9.30	9.56	10.11	13.69
NiO	0.06	0.00	0.00	0.00	0.00	0.00	0.00	0.06	0.03	0.00	0.02
CaO	16.25	15.60	20.62	18.97	22.77	21.67	15.75	16.20	17.16	18.08	22.00
Na_2O	4.39	5.04	2.19	3.40	1.30	1.18	3.72	4.58	3.91	2.89	0.62
K_2O	0.00	0.05	0.02	0.00	0.00	0.04	0.06	0.01	0.01	0.00	0.04
Total	99.10	100.93	100.87	101.99	101.13	99.54	96.44	99.57	99.31	99.64	99.03
Equ. O	6.00	6.00	6.00	6.00	6.00	6.00	6.00	6.00	6.00	6.00	6.00
Si	1.96	2.02	1.90	1.91	1.94	1.87	2.01	1.94	1.91	1.90	1.99
AlIV	0.04	0.00	0.10	0.09	0.06	0.13	0.00	0.06	0.09	0.10	0.01
AlVI	0.33	0.36	0.18	0.23	0.03	0.01	0.42	0.34	0.31	0.27	0.05
Alt	0.37	0.36	0.28	0.32	0.09	0.14	0.42	0.40	0.40	0.37	0.06
Ti	0.00	0.00	0.00	0.01	0.00	0.00	0.00	0.00	0.00	0.00	0.00
Cr	0.00	0.00	0.00	0.00	0.00	0.00	0.00	0.00	0.00	0.00	0.00
Fe3+	0.01	0.00	0.07	0.08	0.12	0.21	0.00	0.03	0.04	0.02	0.00
Fe2+	0.17	0.17	0.18	0.13	0.12	0.04	0.17	0.16	0.17	0.23	0.25
Mg	0.53	0.50	0.60	0.60	0.74	0.80	0.49	0.50	0.52	0.55	0.76
Ni	0.00	0.00	0.00	0.00	0.00	0.00	0.00	0.00	0.00	0.00	0.00
Mn	0.00	0.00	0.00	0.00	0.00	0.00	0.00	0.00	0.00	0.00	0.00
Ca	0.64	0.60	0.81	0.72	0.89	0.86	0.64	0.63	0.67	0.71	0.88
Na	0.31	0.35	0.15	0.24	0.09	0.08	0.27	0.32	0.28	0.21	0.05
K	0.00	0.00	0.00	0.00	0.00	0.00	0.00	0.00	0.00	0.00	0.00
Total	4.00	4.00	4.00	4.00	4.00	4.00	4.00	4.00	4.00	4.00	4.00
XFe	0.25	0.25	0.23	0.18	0.14	0.04	0.25	0.24	0.25	0.29	0.25
Jd	31.06	35.67	15.60	23.07	3.03	0.53	28.69	32.33	27.75	20.61	4.53
Ac	1.19	0.43	3.86	4.91	6.47	18.47	0.30	2.02	2.58	1.36	0.25

* Reconstituted omphacite after average composition of 312 Cpx + Pl symplectite analyses.

content, ranging from $X_{Jd} = 0.23$ to as low as 0.03 where Cpx_2 is in contact with plagioclase (Table 2). To estimate the bulk composition of the Cpx_2 + plagioclase symplectite, a representative area in sample Eg18 was analysed under the electron microprobe by integrating 312 contiguous areas (15 μm × 15 μm) scanned by the electron beam. This bulk composition, when converted to clinopyroxene stoichiometry,

Table 3
Representative electron microprobe data of amphibole.

Sample	Eg18 inclusion	Eg18 matrix (core)	Eg18 matrix (inner rim matrix)	Eg18 (inner rim matrix)	Eg18 (outer rim)	Eg18 corona	Eg82 matrix	Eg82 matrix	Eg82 corona	Eg82 corona
SiO2	36.88	44.62	47.00	47.09	45.65	41.72	44.39	43.51	45.41	43.64
TiO2	1.66	0.46	0.43	0.41	0.30	0.33	0.68	0.60	0.67	1.13
Al2O3	21.52	12.17	11.82	11.05	10.28	14.98	12.47	12.41	10.19	11.32
Cr2O3	0.02	0.04	0.01	0.03	0.09	0.10	0.00	0.03	0.04	0.00
FeO	17.99	12.35	11.55	11.73	13.04	15.23	12.11	12.34	13.17	13.65
MnO	0.13	0.03	0.03	0.06	0.04	0.08	0.04	0.03	0.01	0.07
MgO	6.23	14.02	15.29	15.19	14.45	10.84	13.53	12.88	13.30	12.38
CaO	11.00	11.22	9.94	10.65	11.56	11.83	9.84	10.30	11.09	11.26
Na_2O	2.72	2.65	2.14	2.43	2.31	2.76	2.39	2.58	2.26	2.47
K_2O	0.05	0.56	0.57	0.47	0.44	0.54	0.38	0.41	0.27	0.30
Total	98.21	98.14	98.77	99.11	98.16	98.42	95.83	95.10	96.40	96.21
Equ. O	23.00	23.00	23.00	23.00	23.00	23.00	23.00	23.00	23.00	23.00
Si	5.45	6.40	6.52	6.59	6.55	6.12	6.41	6.41	6.65	6.46
AlIV	2.55	1.60	1.48	1.41	1.45	1.88	1.59	1.59	1.35	1.54
AlVI	1.20	0.46	0.45	0.41	0.29	0.71	0.53	0.57	0.40	0.44
Ti	0.18	0.05	0.05	0.04	0.03	0.04	0.07	0.07	0.07	0.13
Cr	0.00	0.01	0.00	0.00	0.01	0.01	0.00	0.00	0.01	0.00
Fe3+	0.70	0.74	1.31	0.98	0.80	0.49	1.12	0.81	0.63	0.50
Mg	1.37	3.00	3.16	3.17	3.09	2.37	2.91	2.83	2.90	2.73
Fe2+	1.52	0.74	0.03	0.39	0.77	1.38	0.34	0.71	0.98	1.19
Mn	0.02	0.00	0.00	0.01	0.00	0.01	0.00	0.00	0.00	0.01
Ca	1.74	1.72	1.48	1.60	1.78	1.86	1.52	1.63	1.74	1.79
Na	0.78	0.74	0.58	0.66	0.64	0.79	0.67	0.74	0.64	0.71
K	0.01	0.10	0.10	0.08	0.08	0.10	0.07	0.08	0.05	0.06
Total	15.53	15.56	15.15	15.34	15.50	15.51	15.25	15.44	15.43	15.55
XFe	0.53	0.20	0.01	0.11	0.20	0.37	0.10	0.20	0.31	0.30
Na(M4)	0.26	0.28	0.52	0.40	0.22	0.14	0.48	0.37	0.25	0.21
(Na + K)A	0.53	0.56	0.15	0.34	0.50	0.75	0.26	0.44	0.43	0.55

Please cite this article as: Doukkari, S.A., et al., Prograde and retrograde evolution of eclogite from Adrar Izzilatène (Egéré-Aleksod terrane, Hoggar, Algeria) determined from chemical..., Lithos (2014), http://dx.doi.org/10.1016/j.lithos.2014.12.007

Table 4
Representative electron microprobe data of plagioclase.

Sample	Eg18	Eg18	Eg18	Eg18	Eg18	Eg18	Eg18	Eg82	Eg82	Eg82
	Pl/Cpx2	Pl/Cpx2	Pl/Amp	Pl/Amp	Pl/Ep	Pl/Ep	Pl/Cpx3	Plg/Amp	Pl/Amp	Pl/Amp
SiO_2	62.99	57.21	63.05	50.53	60.55	42.08	52.57	62.81	58.85	61.09
Al_2O_3	23.11	26.91	23.01	30.96	24.88	32.12	30.74	23.37	22.56	25.44
TiO_2	0.01	0.13	0.00	0.06	0.02	0.09	0.00	0.02	0.28	0.01
FeO	0.09	0.26	0.15	0.38	0.25	0.86	0.61	0.17	2.80	0.10
MnO	0.00	0.00	0.00	0.00	0.04	0.01	0.01	0.01	0.00	0.01
MgO	0.00	0.39	0.00	0.00	0.00	0.00	0.00	0.00	2.51	0.00
CaO	4.29	10.28	3.84	13.90	6.04	23.90	12.85	4.54	7.01	6.32
Na_2O	9.67	6.27	9.80	4.03	9.05	0.28	4.63	9.53	7.74	8.19
K_2O	0.14	0.09	0.17	0.17	0.25	0.07	0.03	0.11	0.16	0.08
Total	100.30	101.53	100.01	100.03	101.07	99.40	101.45	100.55	101.89	101.24
Equ. O	8.00	8.00	8.00	8.00	8.00	8.00	8.00	8.00	8.00	8.00
Si	2.78	2.54	2.79	2.31	2.68	2.01	2.36	2.77	2.63	2.68
Al	1.20	1.41	1.20	1.67	1.30	1.81	1.63	1.22	1.19	1.32
Ti	0.00	0.00	0.00	0.00	0.00	0.00	0.00	0.00	0.01	0.00
Fe2 +	0.00	0.01	0.01	0.01	0.01	0.03	0.02	0.01	0.10	0.00
Mn	0.00	0.00	0.00	0.00	0.00	0.00	0.00	0.00	0.00	0.00
Mg	0.00	0.03	0.00	0.00	0.00	0.00	0.00	0.00	0.17	0.00
Ca	0.20	0.49	0.18	0.68	0.29	1.22	0.62	0.21	0.34	0.30
Na	0.83	0.54	0.84	0.36	0.78	0.03	0.40	0.82	0.67	0.70
K	0.01	0.01	0.01	0.01	0.01	0.00	0.00	0.01	0.01	0.00
Total	5.03	5.02	5.03	5.04	5.07	5.10	5.03	5.03	5.11	5.01
An	0.20	0.48	0.18	0.66	0.27	0.98	0.61	0.21	0.33	0.30
Ab	0.80	0.52	0.81	0.34	0.72	0.02	0.39	0.79	0.66	0.70
Or	0.01	0.00	0.01	0.01	0.01	0.00	0.00	0.01	0.01	0.00

(analysis Cpx312* in Table 2), approaches that of omphacite (Jd_{28}), indicating that the symplectites are pseudomorphs after omphacite. However, the composition does differ slightly from that of relict omphacite (Cpx_1) in the same sample by its Si content (2.01 p.f.u. instead of 1.96 on average for Cpx_1) and its relatively low jadeite content (X_{Jd} of 0.28 instead of 0.31–0.36). These differences can likely be explained by the non-isochemical character of the omphacite breakdown. The symplectitic clinopyroxene that occurs in coronas replacing amphibole and garnet (Cpx_3 in Fig. 3f) has very low jadeite content (X_{Jd} = 0.005) but has appreciable aegirine solid solution (X_{Aeg} = 0.18; Table 2, Fig. 4c).

4.3. Amphibole

All the grains analysed in the samples are Ca–Na amphiboles, with pargasite and edenite being the most common (Table 3; Fig. 5a,b). Additional sadanagaite or ferro-pargasite is found exclusively as inclusions in garnet. These included grains are characterised by low X_{Mg} of around 0.45, Na(M4) content of 0.28 cations per formula unit (p.f.u.), Si content of 5.50 cations p.f.u and a high Al^{IV} content of 1.40 cations p.f.u (Table 3; Fig. 5a).

Porphyroblastic matrix amphibole grains exhibit complex zoning, with the core to inner rim showing a decrease in X_{Fe}, such that inner rims are edenite with X_{Fe} as low as 0.01 (Table 3; Fig. 5a). The associated Na(M4) content is also high, varying between 0.43 and 0.52 cations p.f.u. Following this zoning, the rims of grains are characterised by a sharp decrease in Na(M4) to between 0.13 and 0.28 cations p.f.u., coupled to Al^{VI} decreasing to between 0.24 and 0.60 cations p.f.u., and X_{Fe} increasing to between 0.10 and 0.28 (Fig. 5a).

The last generation of amphibole occurs in symplectites or coronas around garnet or omphacite and is pargasitic in composition. These grains have the highest X_{Fe} of 0.18 to 0.40, coupled to Al^{VI} contents of 0.30 to 0.60 p.f.u. (Table 3; Fig. 5a).

4.4. Plagioclase

Plagioclase occurs exclusively as a fine-grained phase in symplectites and, as such, has the largest compositional variability of any mineral in the samples. Compositions vary from oligoclase with An_{17} to anorthite with An_{98} (Fig. 5c; Table 4). Plagioclase in symplectites after omphacite has a relatively narrow compositional range between oligoclase (An_{20}) and andesine (An_{47}). Conversely, plagioclase in symplectites developed between garnet and omphacite (Fig. 3c) shows greater variability, with Ca-rich compositions of An_{70} occurring adjacent to garnets and Na-rich compositions of An_{17} occurring towards omphacite. Plagioclase in coronas around epidote also exhibits strong compositional variation, with anorthite (An_{98}) occurring at the epidote boundary, changing to oligoclase with An_{26} towards adjacent amphibole (Figs. 3e and 5c). Finally, plagioclase occurring together with diopside (Cpx_3) has a homogeneous composition of An_{60} (Table 4).

4.5. Epidote

The abundant small grains of epidote found as inclusions in garnet and omphacite have an X_{Fe3+} ratio ($Fe^{3+}/(Fe^{3+}+Al)$) of 0.11 to 0.15. Epidote in the matrix has a lower X_{Fe3+} of 0.07 to 0.12.

5. Interpretation of textures and mineral compositions

The observed reaction textures, coupled to the mineral zoning recorded in porphyroblastic garnet, amphibole and omphacite grains, indicate that progressive stages of metamorphism can be characterised in these rocks. We propose that three distinct development stages along the prograde–peak–retrograde history of these rocks can be identified, namely, a pre-peak stage (M1), the peak eclogite facies stage (M2) and the retrograde stage (M3), with initial decompression resulting in the appearance of plagioclase and the development of kelyphites, prior to the formation of plagioclase + diopside coronas during later retrogression.

The amphibole compositions can trace the continuous evolution of these rocks since it is present during the prograde (in part, M1), peak (M2) and retrograde (M3) stages (Fig. 5d,e). The Na(M4) content of amphibole is the reflection of the amount of glaucophane solid solution (Laird and Albee, 1981) and is sensitive to pressure. Figs. 5d and e are plots of Na(M4) against (Na + K)(A) and $Al^{VI} + Fe^{3+} + Ti$ and show that amphibole inclusions in garnet and the core compositions of porphyroblastic grains reflect relatively low-pressure conditions for M1, similar to data from the Dalradian terrane (Fig. 5d,e; Laird and

Please cite this article as: Doukkari, S.A., et al., Prograde and retrograde evolution of eclogite from Adrar Izzilatène (Egéré-Aleksod terrane, Hoggar, Algeria) determined from chemical..., Lithos (2014), http://dx.doi.org/10.1016/j.lithos.2014.12.007

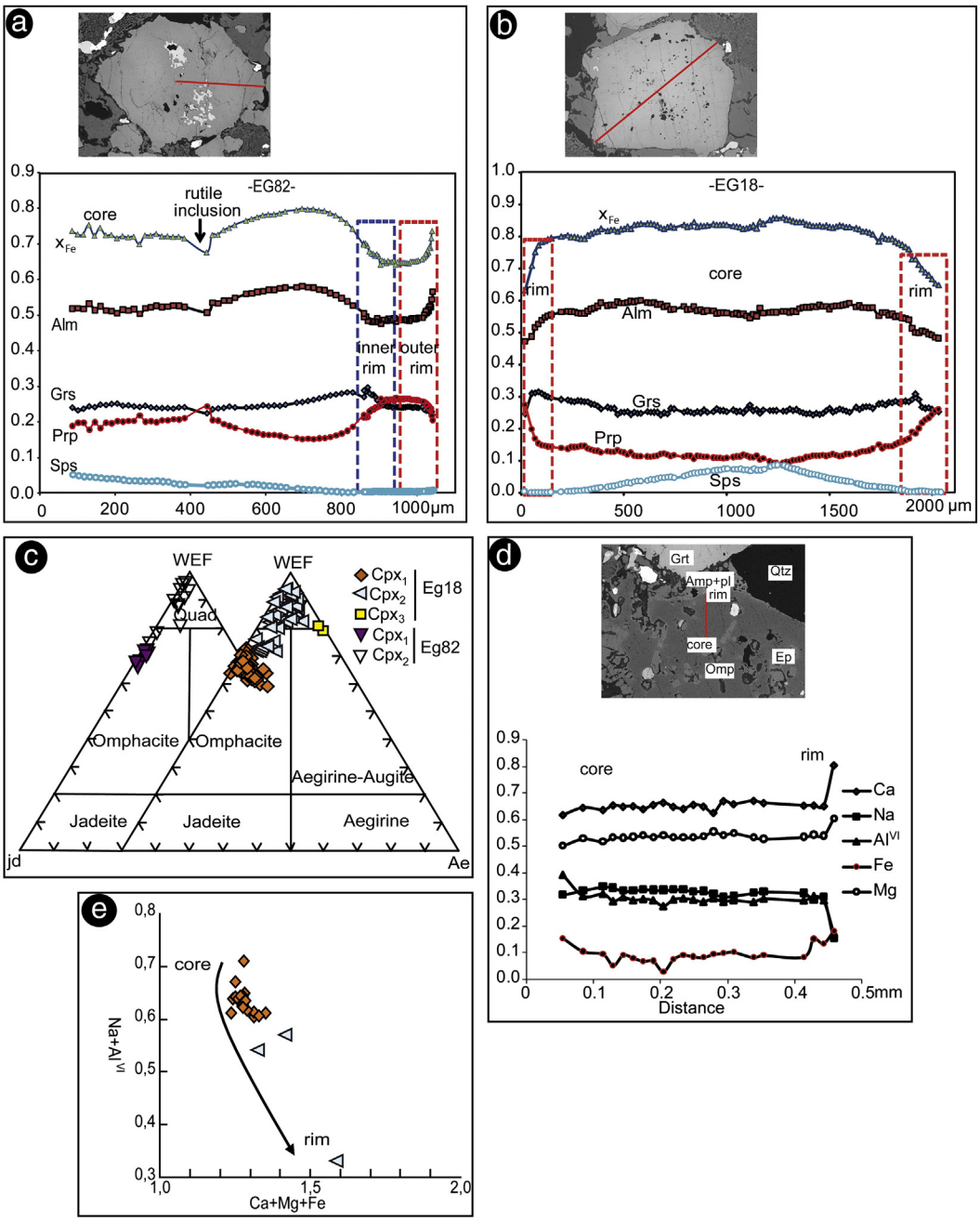

Fig. 4. Diagrams illustrating garnet and clinopyroxene compositions. (a) Garnet zoning profile from sample Eg 82. The core exhibits a flat profile that is almandine-rich and poor in pyrope. The inner rim shows an increase in pyrope content, compensated by a decrease in almandine and grossular. Conversely, the outer rim is richer in almandine and poorer in grossular. (b) Garnet zoning profile from sample Eg18, showing pyrope-rich rim compositions. (c) Clinopyroxene compositions plotted on the aegirine (Ae)–jadeite (Jd)–quadrilateral components (Q) diagram of Morimoto (1988). (d) Omphacite zoning profile, showing a core rich in Na and Al^{VI}, and a marked increase in Ca, Fe and Mg content at the rim adjacent to an amphibole corona. (e) Plot of Na + Al^{VI} vs Ca + Mg + Fe in omphacite, highlighting the core-to-rim reverse jadeite substitution typical of these grains.

Albee, 1981). Conversely, the composition of inner rims reflects higher-pressure conditions during M2, similar to data from the Sanbagawa, Franciscan and Dalradian terranes (Fig. 5d,e; Laird and Albee, 1981). Finally, amphibole rims and grains from symplectites again reflect lower-pressure conditions for M3, similar to data from the Abukuma terrane (Fig. 5d,e; Laird and Albee, 1981).

5.1. Pre-peak stage (M1)

This stage is characterised by epidote, quartz, rutile and calcic amphibole now included within Mg-poor garnet cores. The amphibole is Na(M4)-poor and Al-rich, similar to the inclusions described from garnet cores in eclogite from Nordfjord (Krogh, 1982).

5.2. Peak eclogite facies stage (M2)

The peak metamorphic eclogite facies paragenesis consists of garnet, omphacite, edenite, epidote, rutile and quartz. The large garnet crystals display a zoning with Fe-Ca-rich cores and Mg-rich inner rims (Figs. 3d and 4a, b). The composition of the inner rims from Eg82 and outer rims of Eg18 are taken to reflect the compositions that are in relative equilibrium with the rest of the eclogite paragenesis. Similarly, the jadeite-rich

Please cite this article as: Doukkari, S.A., et al., Prograde and retrograde evolution of eclogite from Adrar Izzilatène (Egéré-Aleksod terrane, Hoggar, Algeria) determined from chemical..., Lithos (2014), http://dx.doi.org/10.1016/j.lithos.2014.12.007

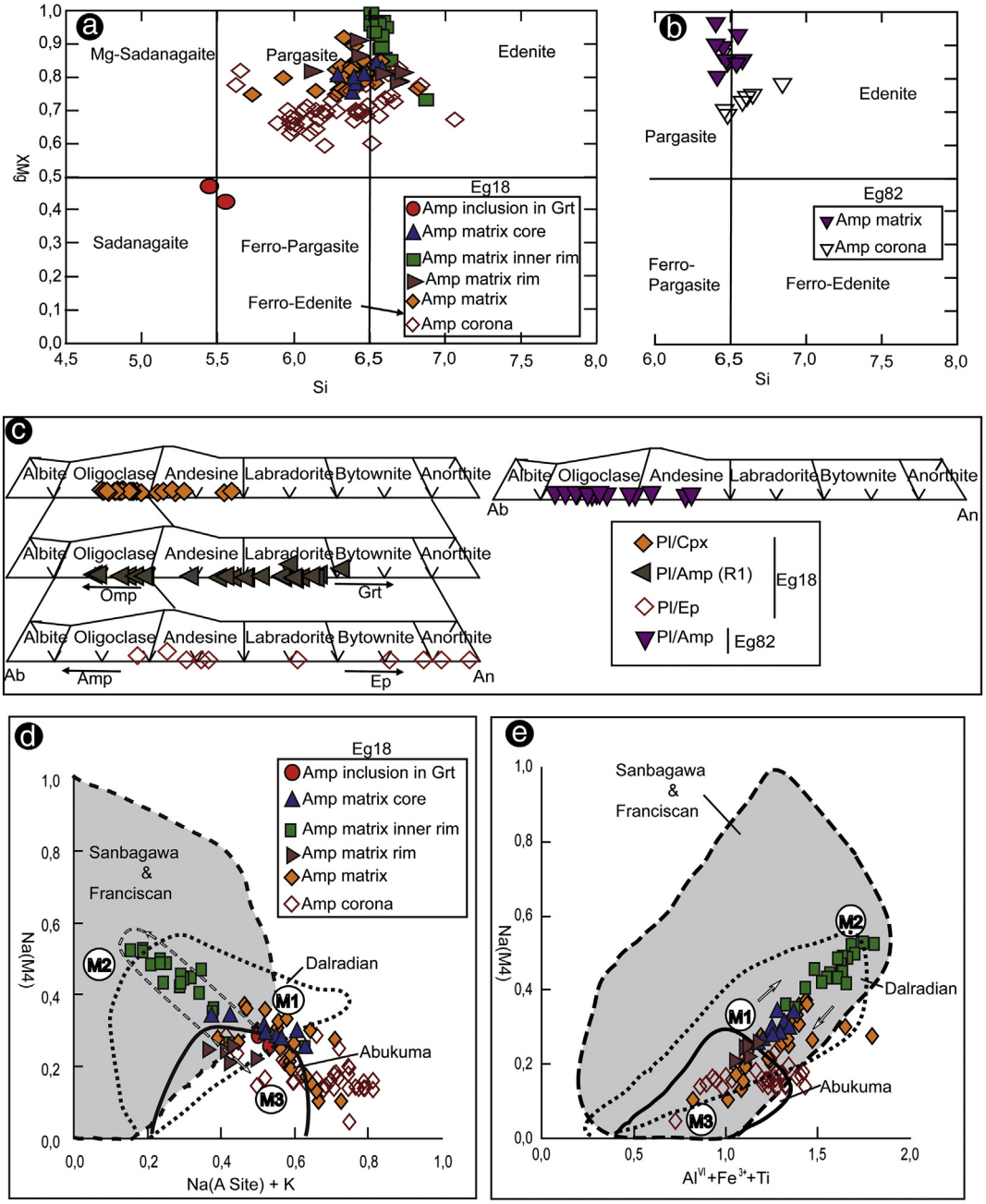

Fig. 5. Diagrams of amphibole and plagioclase compositional variation. (a, b) Amphibole compositions from different textural settings plotted on the diagram of Leake et al. (1997). (c) Plagioclase compositions plotted on the albite–anorthite–orthoclase diagram showing compositional variations for different textural settings. (d) Plot of Na(M4) vs (Na + K)(A) in amphibole from different textural settings, compared to compositions from the Sanbagawa, Franciscan, Dalradian and Abukuma terranes (from Laird and Albee, 1981). The dashed white arrow indicates the compositional change from the M1 to M3 metamorphic stages. (e) Plot of Na(M4) vs $Al^{VI} + Fe^{3+} + Ti$ in amphibole from different textural settings, compared to compositions from the Sanbagawa, Franciscan, Dalradian and Abukuma terranes (from Laird and Albee, 1981). The white arrows indicate the compositional change from the M1 to M3 metamorphic stages.

omphacite and edenite amphibole compositions are taken to reflect peak eclogite facies conditions.

5.3. Retrograde stage (M3)

5.3.1. Symplectite after omphacite

The outer parts of omphacite grains show decreases of Na and Al^{VI} balanced with increases of Fe, Mg and Ca, which is taken to reflect the initiation of retrograde decompression. Omphacite is also transformed into very thin symplectites of diopsidic clinopyroxene (Cpx_2) + plagioclase. The first plagioclase to appear during this stage is albite to oligoclase, associated with newly crystallised clinopyroxene (Cpx_2). This clinopyroxene has lower jadeite content and is slightly enriched in Al^{IV} compared to peak omphacite. The textures suggest that diopside and plagioclase are being produced at the expense of omphacite and quartz.

5.3.2. Kelyphite

Pargasite–plagioclase–ilmenite symplectites formed mainly at the expense of garnet (Grt_1) and omphacite, during a multivariant sliding reaction. The reaction also changed the composition of garnet relicts (Grt_2), and the rims of the initial garnet (Grt_1). The symplectite has a mosaic texture, taken to indicate that it reflects local equilibrium. The reaction responsible for symplectite formation has been balanced

using the method of least squares (see Godard, 2009, and Adjerid et al., 2013 for the algorithm and software used). The compositions of reactant omphacite and average garnet rims, as well as the produced plagioclase, diopsidic clinopyroxene (Cpx_2), re-equilibrated garnet (Grt_2) and amphibole corona compositions from sample Eg18 were used, and yielded a balanced reaction with very low residual (R), indicating that the reaction is nearly isochemical:

5.4. Grt_1 + 2.04 Omp + 0.65 Rt ↔ 0.76 Grt_2 + 1 Pl + 0.05 Amp + 1.34 Cpx_2 + 0.64 Ilm + R

The compositions of reactants and products used are as follows:

$Grt_1 = (Ca_{0.88}Fe_{1.61}Mg_{0.48}Mn_{0.01})(Si_{2.98}Al_{1.95})O_{12}$

$Omp = (Ca_{0.62}Na_{0.31}Mg_{0.50}Fe_{0.15})(Si_2Al_{0.39})O_6$

$Cpx_2 = (Ca_{0.88}Na_{0.05}Mg_{0.73}Fe_{0.27})(Si_2Al_{0.04})O_6$

$Amp = (Ca_{1.71}Na_{0.86}Mg_{2.52}Fe_{0.55})(Si_{5.65}Al_{3.25})O_{23}$

$Grt_2 = (Ca_{0.72}Fe_{1.63}Mg_{0.62}Mn_{0.02})(Si_{2.98}Al_{1.96})O_{12}$

$Pl = (Na_{0.53}Ca_{0.52})Al_{1.48}Si_{2.48}O_8$

$R = Si_{0.01}Al_{0.02}Ti_{0.02}Fe_{0.01}Na_{0.01}Mg_{0.01}Ca_{0.01}O_{-0.001}$

5.4.1. Plagioclase coronas around epidote

Anorthite-rich plagioclase (up to An_{98}) forming coronas around eclogite facies clinozoisite (Fig. 3e; Section 4.4) are interpreted to reflect a retrograde evolution towards lower-pressure and relatively high-temperature conditions.

5.4.2. Plagioclase + diopside coronas around amphibole

The latest stage in the evolution of these rocks resulted in the formation of the most jadeite-depleted clinopyroxene (Cpx_3), intergrown with plagioclase (An_{60}) in coronas around primary amphibole, garnet and quartz. The zoning in amphibole rims in contact with this texture is characterised by a decrease in Al^{VI}, coupled to increases of Fe and sometimes Ti.

6. Mineral equilibria modelling

In order to constrain the prograde (M1) to peak (M2) metamorphic evolution of the Adrar Izzilaténe eclogitic rocks, the whole rock composition of sample Eg18 was determined using XRF analysis at Geo Labs (geosciences laboratory of Canada). The rock developed reaction textures around omphacitic clinopyroxene and garnet during its M3 decompression and retrograde evolution. This indicates that domains of local equilibrium had developed, such that the composition of the whole rock cannot be used to investigate the *P–T* conditions of reacting domains (e.g., Štĭpskà et al., 2005; Groppo et al., 2007; Cruciani et al., 2012). Rather, the effective bulk composition of the reaction domains was determined through the balanced reaction for these domains, and the pseudosection calculated for this composition is used to investigate the development of kelyphites (e.g., Adjerid et al., 2013; Cruciani et al., 2012; Godard, 2009).

Pseudosections were calculated with the computer program THERMOCALC (Powell and Holland, 1988; version 3.33, updated June 2009), using the 2003 updated version of the Holland and Powell (1998) data set (file tc-ds55.txt). Calculations were performed in the Na_2O–CaO–FeO–MgO–Al_2O_3–SiO_2–H_2O-TiO_2–Fe_2O_3 (NCFMASHTO) chemical system, which is currently the most comprehensive and realistic chemical system for investigating mafic rocks. The activity–composition models used in the calculations are as follows: hornblende, actinolite and glaucophane (Diener et al., 2007; updated by Diener and Powell, 2012); omphacite and diopside (Green et al., 2007; updated by Diener and Powell, 2012); garnet (White et al., 2007); epidote (Holland and Powell, 1998); plagioclase (Holland and Powell, 2003); ilmenite (White et al., 2000); and chlorite (Holland and Powell, 1998). Rutile, sphene, quartz and H_2O are pure end-member phases. The amphibole and clinopyroxene models do not explicitly account for K and Ti; however these components are only present in minor amounts in the analysed compositions (Tables 2 and 3) such that the modelling calculations are likely to reliably reproduce the behaviour of these minerals. The analysed whole rock compositions were converted to the model NCFMASHTO system by ignoring the minor amounts of MnO, Cr_2O_3, P_2O_5 and K_2O before converting 15% of the total Fe to Fe^{3+}, within the range typical for the oxidation state of eclogite (Rebay et al., 2010).

Previous studies on eclogite have demonstrated that the phase relations in these rocks, and the occurrence of overprinting amphibolite or granulite facies assemblages, is a function of not only pressure and temperature but also components such as Fe_2O_3 (Ague et al., 2001; Chinner, 1960; Clarke et al., 1989; Diener and Powell, 2010; Rebay et al., 2010) and H_2O (Baldwin et al., 2007; Dziggel et al., 2012; Rebay et al., 2010; Štĭpskà and Powell, 2005). Rebay et al. (2010) quantitatively investigated the role of H_2O on the stability of eclogite assemblages, and found that these rocks might not form 'true' eclogite facies assemblages under fluid-saturated conditions. Rather, fluid-saturated compositions are dominated by amphibole-bearing assemblages with only minor amounts of garnet and omphacite, and it is only once these rocks are taken to be H_2O-undersaturated that their mineralogy is dominated by garnet and omphacite (Rebay et al., 2010). Therefore, P–M_{H2O} pseudosections were constructed in order to explore the effect of H_2O on the phase relations of the inferred peak assemblages, and to evaluate whether the sample was H_2O-saturated during its prograde-to-peak evolution.

6.1. P–M_{H2O} pseudosection

Previous work has determined that the eclogites from Hoggar have experienced temperatures of around 600–750 °C during the eclogite stage (Berger et al., 2014; Derridj et al., 2010; Doukkari et al., 2014). Consequently, the P–M_{H2O} pseudosection was constructed between 5 and 20 kbar at 650 °C, within the range of likely peak eclogite temperature of these rocks (Fig. 6). In the P–M_{H2O} diagram, the abscissa axis ranges from the dry composition of the bulk rock to a composition that allows H_2O-saturated assemblages over the entire pressure range of interest, with H_2O content ranging from 0 to 5.5 mol%.

At H_2O-saturated conditions, a sequence of mineral changes can be identified for a prograde increase in pressure from 7 to 10 kbar. First, epidote is introduced at the expense of plagioclase, before sphene is replaced by rutile, and finally garnet is stabilised (Fig. 6). However, the sequence is different for H_2O-undersaturated conditions, with garnet being present in all fields except at very low pressure (Fig. 6). With increasing pressure, ilmenite is first replaced by rutile at ~9 kbar, before epidote is introduced at the expense of plagioclase at around 11–14 kbar. The inferred peak assemblage of garnet–omphacite–epidote–hornblende–quartz–rutile is stable at both H_2O-saturated and H_2O-undersaturated conditions for pressures above ~13 kbar (Fig. 6). This suggests that the sample could potentially have been fluid-saturated or -undersaturated during its prograde-to-peak evolution. However, the occurrence of epidote and rutile inclusions in garnet indicates that these minerals were present when garnet was introduced, which requires H_2O-saturated conditions (Fig. 6). If these rocks evolved at H_2O-undersaturated conditions, the garnet inclusion assemblage should include ilmenite and plagioclase. Consequently, it seems appropriate to assume H_2O saturation during the prograde-to-peak evolution of these rocks, allowing it to be constrained through modelling on a H_2O-saturated *P–T* pseudosection.

Please cite this article as: Doukkari, S.A., et al., Prograde and retrograde evolution of eclogite from Adrar Izzilatène (Egéré-Aleksod terrane, Hoggar, Algeria) determined from chemical..., Lithos (2014), http://dx.doi.org/10.1016/j.lithos.2014.12.007

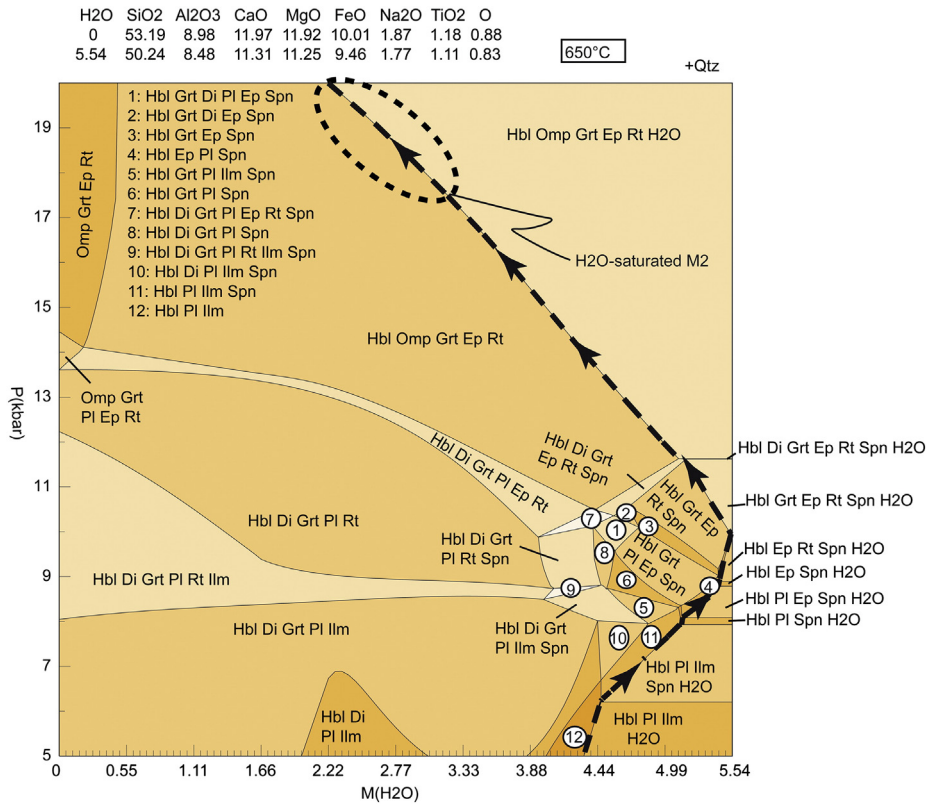

Fig. 6. *P*–M_{H2O} pseudosection for sample Eg18, calculated between 5 and 20 kbar at 650 °C, with M_{H2O} ranging from 0 to 5.54 mol%. The dashed circle indicates the likely conditions of M2 metamorphism, and the dashed arrow indicates the prograde path followed by a H_2O-saturated rock. Mineral abbreviations are after Kretz (1983).

6.2. H_2O-saturated pseudosection

The fluid-saturated pseudosection for sample Eg18 is presented in Fig. 7a. It is calculated from 5 to 22 kbar and 500 to 750 °C. At higher temperature, the assemblages are likely to be metastable with respect to silicate melt, which cannot be reproduced in the modelling because an appropriate melt model is not available (e.g., White et al., 2007). The pseudosection is characterised by amphibole-bearing assemblages, with glaucophane and actinolite present at low-temperature–high-pressure conditions, and hornblende occurring over the remainder of the *P*–*T* range. Diopsidic and omphacitic clinopyroxenes are calculated to coexist over a small *P*–*T* range at 16–17 kbar and 610–630 °C, but the solvus between the two closes, such that only one hypersolvus clinopyroxene, exists at higher temperatures. Here, the transition from diopside to omphacite occurs through a continuous change in composition, with diopsidic clinopyroxene (with $j(Cpx) = Na/(Na + Ca) < 0.36$) occurring at pressures below 17–18 kbar, whereas omphacitic clinopyroxene (with $j(Cpx) > 0.36$) is calculated to be stable above 17–18 kbar (Fig. 7a). Consequently, the inferred peak eclogite facies assemblage is stable above 17–18 kbar, at between 600 and 750 °C (Fig. 7a). The peak assemblage is bordered to lower pressure by several garnet-, hornblende- and plagioclase-bearing assemblages.

The inferred prograde assemblage containing hornblende, rutile and epidote in the presence of garnet occurs at temperatures above 570 °C and pressures above 10.5 kbar (Fig. 7a). It is bounded to lower temperatures by the presence of chlorite and to lower pressures by the absence of garnet. It is bordered by the peak metamorphic assemblage to higher *P*–*T* conditions (Fig. 7a).

To explain the garnet zoning, the garnet-bearing assemblage fields are contoured for $x(Grt) = Fe/(Fe + Mg)$ and $z(Grt) = Ca/(Ca + Fe + Mg)$ (Fig. 7a). In the field of the inferred prograde assemblage, between 11–18 kbar and 570–640 °C, the isopleths of $z(Grt)$ are strongly dependent on temperature, and only show a slight increase from 0.28 to 0.32 towards high pressure (Fig. 7a). Over the same pressure interval, $x(Grt)$ decreases from 0.85 to 0.80 (Fig. 7a). These compositions are consistent with the compositions analysed from the cores of garnet porphyroblasts (Grt1 to Grt2; Fig. 7b), indicating that the core compositions might reflect a prograde evolution from conditions of ~13.6 kbar and ~570 °C (the point labelled Grt1 on Fig. 7a), to conditions of 17 kbar at 600 °C (the point labelled Grt2 on Fig. 7a). Within the field of the peak assemblage, both $x(Grt)$ and $z(Grt)$ isopleths are primarily dependent on pressure, and both show decreasing values towards high pressure (Fig. 7a). This trend is observed in the rims of garnet zoning profiles (Grt3; Fig. 7b), indicating that they record continuous garnet growth with increasing pressure, from conditions of 17 kbar at 600 °C (the point labelled Grt2 on Fig. 7a) to ~19 kbar at 650–700 °C (the area labelled Grt3 in Fig. 7a).

The prograde path derived from the garnet zoning pattern is further supported by the inclusions found inside garnet crystals, where only hornblende, epidote, rutile and quartz are observed, as well as the analysed amphibole compositions (Fig. 8). Compositional isopleths of $x(Hbl) = Fe/(Fe + Mg)$, $a(Hbl) = Na(A)$, $y(Hbl) = Al^{VI}$, and $z(Hbl) = Na(M4)$ were calculated for the peak metamorphic fields (Fig. 8a,b). The compositions of amphibole inclusions in garnet (Amp M1) are consistent with pre-eclogite prograde conditions of ~14 kbar and 590 °C (Fig. 8a, b), whereas the zonation of the coarse-grained amphibole crystals in the matrix (Amp M2) record a prograde path from core to inner rim (Fig. 8c). The cores of matrix amphibole grains indicate conditions of 17–19 kbar and 630–650 °C (labelled AmpM2 core in Fig. 8a,b), whereas the rims reflect conditions of around 21 kbar and 620–680 °C (labelled AmpM2 rim in Fig. 8a,b). This pseudosection is also contoured for $j(Cpx) = Na/(Na + Ca)$, and the maximum analysed X_{Jd} values of ~ 0.36 constrains peak pressure around 19 kbar and 650–700 °C (Fig. 7a). This highest value of X_{Jd} is considered to have equilibrated with the average garnet rim composition ($x(Grt) = 0.63–0.65$; $z(Grt) = 0.25–0.28$) and rims of matrix amphibole ($x(Hbl) = 0.10–0.15$, $z(Hbl) = 0.35–0.40$).

Please cite this article as: Doukkari, S.A., et al., Prograde and retrograde evolution of eclogite from Adrar Izzilatène (Egéré-Aleksod terrane, Hoggar, Algeria) determined from chemical..., Lithos (2014), http://dx.doi.org/10.1016/j.lithos.2014.12.007

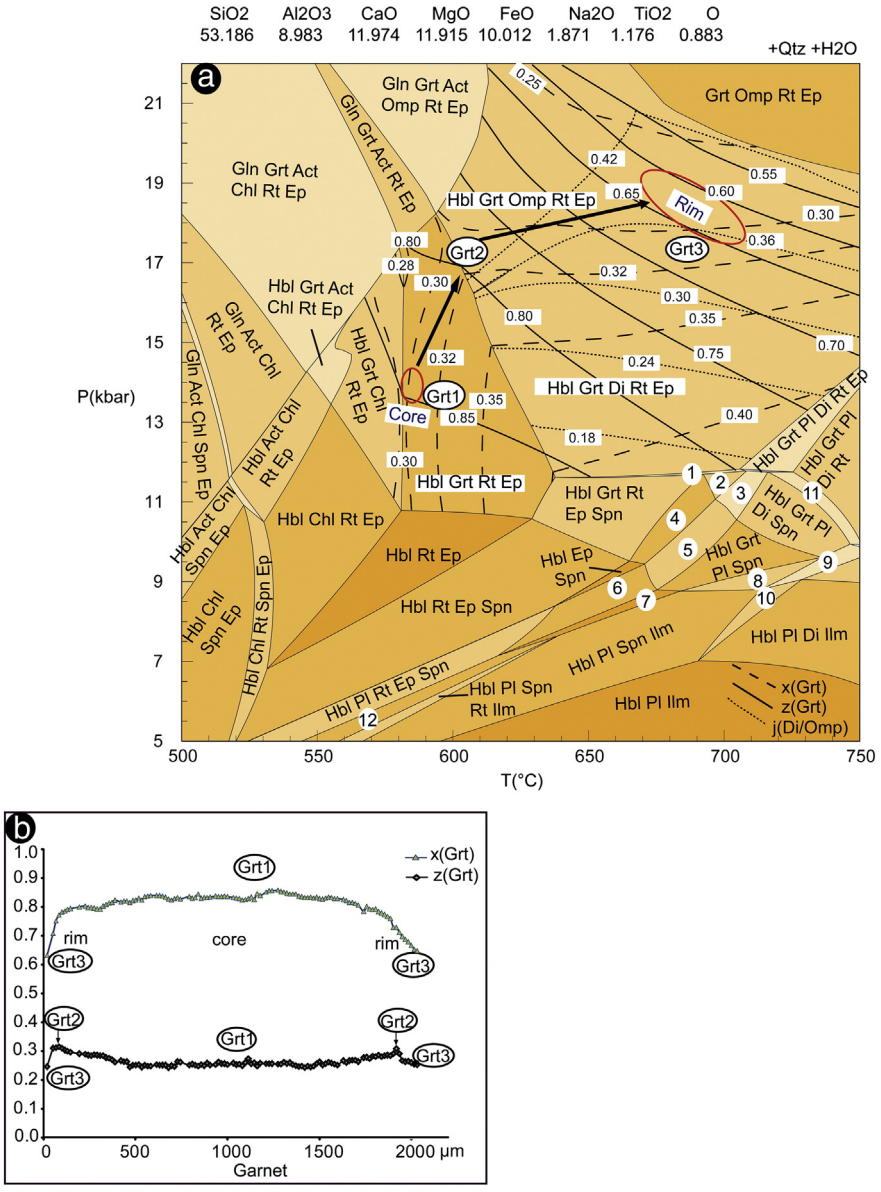

Fig. 7. (a) *P–T* pseudosection for sample Eg18, assuming H_2O saturation and contoured for isopleths of x(Grt) = Fe/(Fe + Mg) and z(Grt) = Ca/(Ca + Fe + Mg) in garnet, and j(Omp) = Na/(Ca + Na) in omphacite. The ellipses represent the metamorphic conditions obtained by the intersection of isopleths from analysed garnet compositions, shown in b. The inferred prograde path is represented by a thick black line. 1: Hbl Grt Di Rt Spn Ep, 2: Hbl Grt Di Spn Ep, 3: Hbl Grt Di Pl Spn Ep, 4: Hbl Grt Spn Ep, 5: Hbl Grt Pl Spn Ep, 6: Hbl Pl Spn Ep, 7: Hbl Pl Spn, 8: Hbl Pl Spn Ilm, 9:Hbl Grt Pl Di Spn Ilm, 10: Hbl Pl Di Spn Ilm, 11: Hbl Grt Pl Di Rt Spn, 12: Hbl Pl Rt Spn. (b) Analysed garnet zoning profile, allowing for comparison with the isopleths calculated in a.

6.3. Modelling the symplectite and the corona stage

The preservation of near-peak mineral assemblages in subsolidus rocks requires the rocks to become fluid-absent early during their retrograde history (Guiraud et al., 2001). Consequently, it is necessary to calculate a new pseudosection, with a fixed H_2O content, to constrain details of the retrograde path. In order to examine the development of reaction textures in micro-domain compositions, the composition of these domains was estimated from the balanced reaction 1.23 Grt_1 + 2.04 Omp + 0.65 Rt → 0.76 Grt_2 + 1 Pl + 0.05 Amp + 1.34 Di + 0.64 Ilm (see Section 5.3.2). The amount of H_2O that may have been present in this compositional domain was estimated based on the abundance of amphibole—being the main hydrous mineral—in the sample. The bulk composition used for the pseudosection in Fig. 9 is (in mol%): H_2O = 0.98, SiO_2 = 48.76, Al_2O_3 = 9.29, CaO = 13.65, MgO = 9.36, FeO = 13.33, Na_2O = 1.84, TiO_2 = 1.90, Fe_2O_3 = 0.85. The pseudosection is contoured for isopleths of j(Di/Omp) = Na/(Na + Ca) and x(Di/Omp) = Fe/(Fe + Mg) in clinopyroxene (Fig. 9b), y(Hbl) = Al^{VI}, z(Hbl) = Na(M4) and x(Hbl) = Fe/(Fe + Mg) for amphibole (Fig. 9c), and ca(Pl) = Ca/(Ca + Na) for plagioclase (Fig. 9b).

Plagioclase is calculated to not be stable at peak conditions but is introduced at around 13 kbar, upon decompression in the H_2O-free fields. With decreasing pressure, plagioclase becomes more anorthite-rich and clinopyroxene becomes less jadeitic (Fig. 9b). The appearance of ilmenite at the expense of rutile, and the stability of the M3 symplectic assemblage, occurs in the relatively narrow pressure interval between 7 and 9 kbar over the entire temperature range considered (Fig. 9a). The intersection of the average analysed mineral compositions (j(Di) = 0.15, x(Di) = 0.23, z(Hbl) = 0.45, x(Hbl) = 0.30, y(Hbl) = 0.45, ca(Pl) = 0.50) occurs at conditions of 8–9 kbar and 700–750 °C (the area labelled kelyphite M3 in Fig. 9a) and are taken to reflect the conditions under which the textures most likely developed. Consequently, a retrograde path from peak metamorphism to the conditions of symplectite formation can be inferred (arrow in Fig. 9a).

Please cite this article as: Doukkari, S.A., et al., Prograde and retrograde evolution of eclogite from Adrar Izzilatène (Egéré-Aleksod terrane, Hoggar, Algeria) determined from chemical..., Lithos (2014), http://dx.doi.org/10.1016/j.lithos.2014.12.007

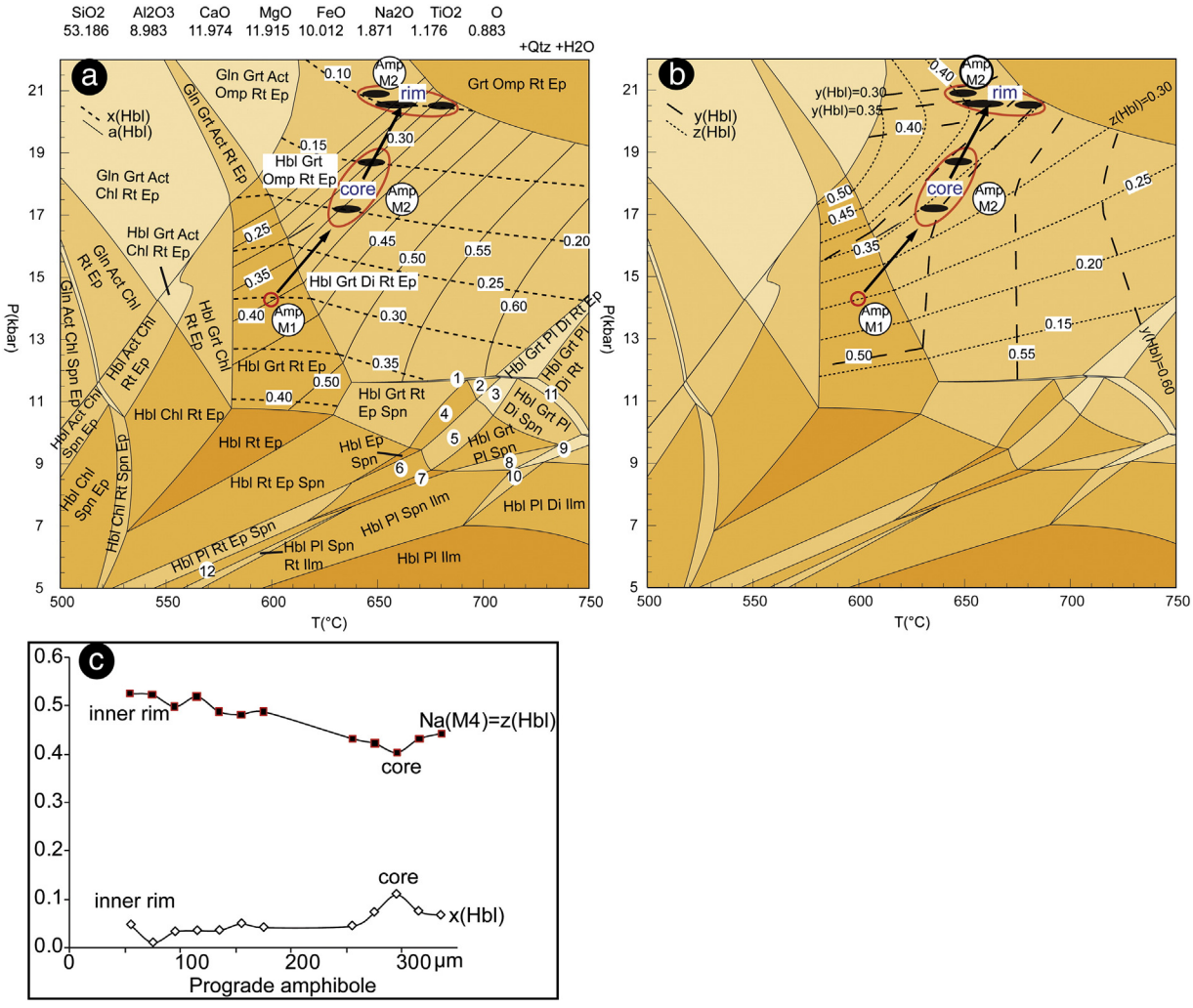

Fig. 8. *P–T* pseudosection for sample Eg18, assuming H_2O saturation and contoured for isopleths of (a) $x(Hbl) = Fe/(Fe + Mg)$ and $a(Hbl) = X_{Na}(A)$ and (b) $y(Hbl) = Al^{VI}$ and $z(Hbl) = X_{Na}(M4)$ in amphibole. The ellipses represent the metamorphic conditions obtained by the intersection of isopleths from analysed amphibole compositions, shown in b. The inferred prograde path is represented by a thick black line. Labels 1–12 are as in Fig. 7(a). (c) Analysed amphibole zoning profile, allowing comparison with the isopleths calculated in a and b.

7. Discussion and conclusion

7.1. The role of retrograde fluid and deformation

During the analysis of metamorphic rocks, the concept of equilibrium may be applied locally at the grain-boundary scale (e.g., Powell, 1978), and in this paradigm, the preserved mineralogy must be viewed as a series of attempts to reach new equilibrium. Similarly, the preservation of peak metamorphic assemblages depends on the absence of hydrous fluid infiltration during exhumation (Guiraud et al., 2001). In the samples from Adrar Izzilatène, the limited retrograde replacement of omphacite suggests that H_2O availability during exhumation was restricted (Zheng et al., 2003), and that the most anhydrous, highest-pressure assemblages are preserved (Zhang and Liou, 1997). The most likely fluid source responsible for the limited retrogression is primary amphibole (Amp M2) and epidote, whose breakdown during decompression-heating may have led to very local retrogression in eclogite. In addition, the CO_2-rich marbles that are associated with, and envelop the eclogite lenses, could have further aided their preservation by providing an effective buffer against external fluid flux.

The rates of metamorphic re-equilibration increase in the presence of deformation, such that deforming mafic rocks will more easily equilibrate to high-pressure metamorphic conditions (e.g., Austrheim and Griffin, 1985; Austrheim et al., 1998) but will also be more readily affected by retrogression (Doukkari et al., 2014; Koons et al., 1987; Sautter, 1985; Zetoutou et al., 2004). The lack of penetrative deformation fabrics in the studied samples is likely to have inhibited the development of retrograde assemblages, while also limiting the extent of fluid infiltration. The lack of deformation can be explained by the enveloping marbles, which would have provided a locus for exhumation-related deformation, thereby shielding the eclogite from recrystallisation.

7.2. Comparison with other eclogite occurrences, and implications for the crustal evolution of Hoggar

The Izzilatène eclogite provides important geodynamic constraints on the evolution of the LATEA metacraton. However, without precise age and isotopic data it is premature to propose a comprehensive geodynamic model. The age of the protoliths to the Hoggar eclogites is contentious, as eclogites from various localities in the LATEA metacraton are recognised to have either Archaean–Paleoproterozoic or Neoproterozoic protolith ages (Bernard-Griffiths et al., 1991; Liégeois et al., 2003). The interpretation of Archaean–Paleoproterozoic protolith ages is not unequivocal, and it has been argued that the high $^{147}Sm/^{144}Nd$ ratios of ~ 0.19 in these rocks precludes the calculation of meaningful Nd T_{DM} model ages (see Liégeois and Stern, 2010 and Stern, 2002). For eclogite occurrences where the protoliths appear to belong to the Archaean–Paleoproterozoic basement, the eclogitic parageneses have been linked to reworking of the rocks along Pan-African

Please cite this article as: Doukkari, S.A., et al., Prograde and retrograde evolution of eclogite from Adrar Izzilatène (Egéré-Aleksod terrane, Hoggar, Algeria) determined from chemical..., Lithos (2014), http://dx.doi.org/10.1016/j.lithos.2014.12.007

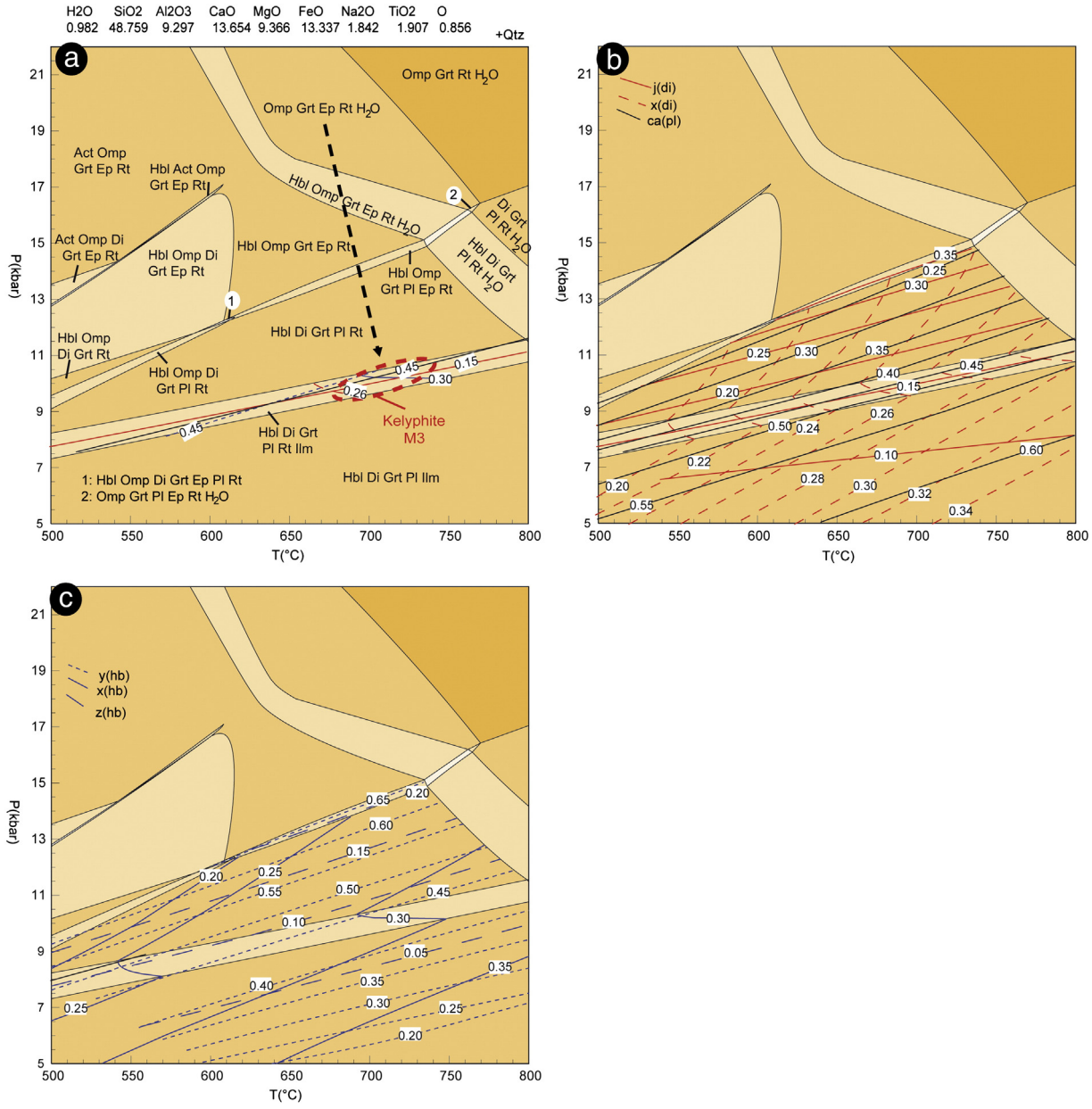

Fig. 9. (a) *P–T* pseudosection calculated for the effective bulk composition of reaction domains in sample Eg18, and contoured for compositional isopleths of (b) $j(\mathrm{Di}) = \mathrm{Na}/(\mathrm{Na} + \mathrm{Ca})$ and $x(\mathrm{Di}) = \mathrm{Fe}/(\mathrm{Fe} + \mathrm{Mg})$ in clinopyroxene, and $\mathrm{ca(Pl)} = \mathrm{Ca}/(\mathrm{Na} + \mathrm{Ca})$ in plagioclase and (c) $y(\mathrm{Hbl}) = \mathrm{Al^{VI}}$, $x(\mathrm{Hbl}) = \mathrm{Fe}/(\mathrm{Fe} + \mathrm{Mg})$ and $z(\mathrm{Hbl}) = \mathrm{X_{Na}(M4)}$ in amphibole. The ellipse in panel a represents the metamorphic conditions estimated from the analysed compositions of the M3 kelyphite assemblage ($\mathrm{ca(Pl)} = 0.45$),$j(\mathrm{Di}) = 0.15$, $x(\mathrm{Jd}) = 0.26$, $y(\mathrm{Hbl}) = 0.45$, $x(\mathrm{Hbl}) = 0.30$).

structures (Sautter, 1985, 1986). Conversely, for examples where the eclogites were derived from juvenile protoliths, such as at Tidéridjaouine (Berger et al., 2014), it has been demonstrated that the rocks originated as basalts formed 700–800 Ma ago in a continental rift that evolved to an oceanic basin, before experiencing eclogite facies metamorphism at 623 ± 3 Ma (Berger et al., 2014).

Therefore, irrespective of the age and origin of the protolith, the eclogite facies metamorphism is always recognised to be Neoproterozoic in age, and to have occurred during the convergent stages of the Pan-African orogeny (Berger et al., 2014; Bernard-Griffiths et al., 1991; Liégeois et al., 2003). The age of eclogite facies metamorphism for the Izzilatène eclogites described here is therefore more than likely to also be Neoproterozoic. The presence of the Izzilatène eclogite at the contact between the Paleoproterozoic Arechchoum and Egéré Series, as well as high-strain deformation fabrics indicates that these rocks are associated with a major thrust fault.

Three possible scenarios are proposed to explain the evolution of these rocks:

(1) If one assumes a Paleoproterozoic protolith as well as a Paleoproterozoic age for eclogite metamorphism, that would relate their entire evolution to the Eburnian orogeny. This would be the first documented case for Eburnian eclogites in the Tuareg Shield and appears highly unlikely when one considers that documented Eburnian metamorphism involves ultra-high temperature (Ouzegane et al., 2003) or at least granulite facies conditions (Bendaoud et al., 2008; Peucat et al., 2003).

(2) Assuming a Paleoproterozoic protolith and Pan-African age for eclogitic metamorphism would indicate the continental subduction of the Egéré-Aleksod terrane, during the Neoproterozoic metacratonic evolution of LATEA.

Please cite this article as: Doukkari, S.A., et al., Prograde and retrograde evolution of eclogite from Adrar Izzilatène (Egéré-Aleksod terrane, Hoggar, Algeria) determined from chemical..., Lithos (2014), http://dx.doi.org/10.1016/j.lithos.2014.12.007

(3) If one assumes a Neoproterozoic oceanic protolith and Pan-African age for eclogitic metamorphism, that would correlate the evolution of the Izzilatène eclogite to that of the Tin Begane eclogite (Liégeois et al., 2003) as well as the eclogitised oceanic material of the Ti-N-Eggoleh area (Adjerid et al., in this volume). Liégeois et al. (2003) considered that all the eclogitic units in central LATEA (locations I, II, III in Fig. 1b) might belong to a single oceanic domain, and proposed that they can be used as markers to estimate the amount of post-collisional horizontal displacement experienced by various terranes inside LATEA. Using this, Liégeois et al. (2003) estimated maximum displacements of 500 km, and related it to the period of northwards-directed escape when LATEA was squeezed between the West African craton and Saharan metacraton. If this were the case, it would imply that the protoliths to the Izzilatène eclogite were part of a former ocean that was located to the west of LATEA.

Scenarios 2 and 3 are not incompatible, as the former passive margin of LATEA had to have been subducted in order to accrete oceanic rocks or sediments from the former active margin. A similar history has been recognised in the Norwegian Caledonides (Hacker et al., 2010; Küllerud et al., 2001; Lappin and Smith, 1978). In such a model, evolution from the prograde conditions reached during M1 (13–14 kbar, 580 ± 30 °C) to peak conditions reached during M2 (19 kbar, 650–700 °C) can be achieved during either oceanic or continental subduction. However, retrogression to lower-pressure conditions during M3 (8–9 kbar at around 700–750 °C) was achieved by near-isothermal decompression, which is characteristic of continental exhumation following subduction (e.g., England and Thompson, 1984). An important consequence of this model is that, whatever scenario is considered, the evolution of these rocks can be explained without the need for lithospheric thickening, which is a typical characteristic for the accretionary evolution of a metacraton (Liégeois et al., 2013).

Acknowledgements

We sincerely thank Geoffrey Clarke and the anonymous reviewer for their constructive reviews and for improving the manuscript. L. Gordon Medaris and Daniele Castelli are thanked for their editorial handling. This work is a contribution to the project PHC TASSILI «Imagerie et Modélisation géologique et géophysique du Hoggar: Implications géodynamiques et Métallogéniques» and CNEPRU program «Modélisation thermodynamique et implication géodynamique des zones de suture de haute pression du Hoggar».

References

Abdallah, N., Liégeois, J.P., De Waele, B., Fezaa, N., Ouabadi, A., 2007. The Temaguessine Fe-cordierite orbicular granite (Central Hoggar, Algeria): U–Pb SHRIMP age, petrology, origin and geodynamical consequences for the late Pan-African magmatism of the Tuareg shield. Journal of African Earth Sciences 49, 153–178.

Acef, K., Liégeois, J.P., Ouabadi, A., Latouche, L., 2003. The Anfeg post-collisional Pan-African high-K calc-alkaline batholith (Central Hoggar, Algeria), result of the Latea microcontinent metacratonisation. Journal of African Earth Sciences 37, 295–311.

Adjerid, Z., Ouzegane, K., Godard, G., Derridj, A., Kienast, J.R., 2012. Le Sérouènout : un fragment de lithosphère océanique subducté à haute pression, exhumé puis granulitisé à haute température. Bulletin du Service Géologique National 23 (3), 199–217.

Adjerid, Z., Godard, G., Ouzegane, K., Kienast, J.R., 2013. Multistage evolution of unusual osumilite-bearing assemblages preserved in ultrahigh-temperature granulites from In Ouzzal (Hoggar, Algeria). Journal of Metamorphic Geology 31, 505–524.

Adjerid, Z., Godard, G., Ouzegane, K., 2014. High-pressure whiteschists from the Ti-N-Eggoleh area (Central Hoggar, Algeria): Record of the Pan-African oceanic subduction. Lithos (in this volume).

Ague, J.J., Baxter, E.F., Eckert, J.O., 2001. High fO_2 during sillimanite zone metamorphism of part of the Barrovian type locality, Glen Clova, Scotland. Journal of Petrology 42, 1301–1320.

Arab, A., Ouzegane, K., Drareni, A., Doukkari, S., Zetoutou, S., Kienast, J.R., 2014. Phase equilibria modeling of kyanite-bearing eclogitic metapelites in the NCKFMASHTO system from the Egere terrane (Central Hoggar, South Algeria). Arabian Journal of Geosciences http://dx.doi.org/10.1007/s12517-014-1413-z (online).

Austrheim, H., Griffin, W.L., 1985. Shear deformation and eclogite formation within granulite-facies anorthosites of the Bergen Arcs, Western Norway. Chemical Geology 50, 267–281.

Austrheim, H., Erambert, M., Engvik, A.K., 1998. Processing of crust in the root of the Caledonian continental collision zone: The role of eclogitisation. Tectonophysics 273, 129–153.

Baldwin, J.A., Powell, R., Williams, M.L., Goncalves, P., 2007. Formation of eclogite, and reaction during exhumation to mid-crustal levels, Snowbird tectonic zone, western Canadian Shield. Journal of Metamorphic Geology 25, 953–974.

Barbey, P., Bertrand, J.M.L., Angoua, S., Dautel, D., 1989. Petrology and U/Pb geochronology of the Telohat migmatites, Aleksod, Central Hoggar, Algeria. Contributions to Mineralogy and Petrology 101, 207–219.

Bendaoud, A., Derridj, A., Ouzegane, K., Kienast, J.R., 2004. Granulites of the Laouni terrane, (Tamanrasset, Tidjenouine, Tin Begane). Journal of African Earth Sciences 39, 187–192.

Bendaoud, A., Ouzegane, K., Godard, G., Liégeois, J.P., Kienast, J.R., Bruguier, O., Drareni, A., 2008. The Eburnian Granulitic Metapelites of Tidjenouine, geochronology and metamorphic P-T-X evolution: Witness of the LATEA metacratonic evolution (Central Hoggar, Algeria). Geological Society,London, Special Publications 'Boundaries of the West African Craton 297, 111–146.

Berger, J., Caby, R., Liégeois, J.P., Mercier, J.C., Demaiffe, D., 2011. Deep inside a Neoproterozoic intra-oceanic arc: Growth, differentiation and exhumation of the Amalaoulaou complex (Gourma, Mali). Contributions to Mineralogy and Petrology 162, 773–796.

Berger, J., Ouzegane, K., Bendaoud, A., Liégeois, J.P., Kienast, J.R., Bruguier, O., Caby, R., 2014. Continental subduction recorded by Neoproterozoic eclogite and garnet amphibolites from Western Hoggar (Tassendjanet terrane, Tuareg Shield, Algeria). Precambrian Research 247, 139–158.

Bernard-Griffiths, J., Peucat, J.J., Ménot, R.-P., 1991. Isotopic (Rb-Sr, U-Pb and Sm-Nd) and trace element geochemistry of eclogites from the pan-African belt: A case study of REE fractionation during high grade metamorphism. Lithos 27, 43–57.

Bertrand, J.M.L., 1974. Evolution polycylique des gneiss précambriens de l'Aleksod (Hoggar central, Sahara Algérien). Thèse d'Etat, In: C.N.R.S. (C.R.Z.A) (Ed.), Aspects structuraux, pétrologiques, géochimiques et géochronologiques. série géologique 19 (350 pp.).

Bertrand, J.M.L., Caby, R., 1978. Geodynamic evolution of the Pan-African orogenic belt; a new interpretation of the Hoggar Shield (Algerian Sahara). Geologische Rundschau 67, 357–388.

Bertrand, J.M.L., Michard, A., Boullier, A.M., Dautel, D., 1986. Structure and U/Pb geochronology of central Hoggar (Algeria); a reappraisal of its Pan-African evolution. Tectonics 5, 955–972.

Black, R., Latouche, L., Liégeois, J.P., Caby, R., Bertrand, J.M., 1994. Pan-African displaced terranes in the Tuareg Shield (Central Sahara). Geology 22, 641–644.

Caby, R., 1996. A review of the In Ouzzal granulitic terrane (Tuareg shield, Algeria): Its significance within the Pan-African Trans-Saharan belt. Journal of Metamorphic Geology 14, 659–666.

Caby, R., 2003. Terrane assembly and geodynamic evolution of Central-Western Hoggar: A synthesis. Journal of African Earth Sciences 37, 133–159.

Caby, R., Andréopoulos-Renaud, U., 1987. The Eastern Hoggar, 730 Ma Old Cratonic Block in the Pan-African Belt of the North African Continent. Precambrian Research 36, 335–344.

Caby, R., Monié, P., 2003. Neoproterozoic subductions and differential exhumation of western Hoggar (southwest Algeria): New structural, petrological and geochronological evidence. Journal of African Earth Sciences 37, 269–293.

Caby, R., Andréopoulos-Renaud, U., Pin, C., 1989. Late Proterozoic arc-continent and continent-continent collision in the Pan-African Trans-Saharan Belt of Mali. Canadian Journal of Earth Sciences 26, 1136–1146.

Cahen, L., Snelling, N.J., Delhal, J., Vail, R.J., 1984. The geochronology and evolution of Africa. Clarendon Press, Oxford (512 pp.).

Carson, C.J., Powell, R., Clarke, G.L., 1999. Calculated mineral equilibria for eclogites in $CaO–Na_2O–FeO–MgO–Al_2O_3–SiO_2–H_2O$: Application to the Poue´bo Terrane, Pam Peninsula, New Caledonia. Journal of Metamorphic Geology 17, 9–24.

Chinner, G.A., 1960. Pelitic gneisses with varying ferrous/ferric ratios from Glen Clova, Angus, Scotland. Journal of Petrology 1, 178–217.

Clarke, G.L., Powell, R., Guiraud, M., 1989. Low-pressure granulite metapelitic assemblages and corona textures from MacRobertson Land, east Antarctica: The importance of Fe_2O_3 and TiO_2 in accounting for spinel bearing assemblages. Journal of Metamorphic Geology 7, 323–335.

Cruciani, G., Franceschelli, M., Groppo, C., Spano, M.E., 2012. Metamorphic evolution of non-equilibrated granulitised eclogite from Punta de li Tulchi (Variscan Sardinia) determined through texturally controlled thermodynamic modelling. Journal of Metamorphic Geology 30, 667–685.

Derridj, A., Ouzegane, K., Adjerid, Z., Godard, G., Kienast, J.R., 2010. Les éclogites granulitisées de Tin-Eggoleh (terrane du sérouènout, Hoggar Central): Étude métamorphique et conséquence géodynamique. Bulletin du Service Géologique National 21 (2), 117–136.

Diener, J.F.A., Powell, R., 2010. Influence of ferric iron on the stability of mineral assemblages. Journal of Metamorphic Geology 28, 599–613.

Diener, J.F.A., Powell, R., 2012. Revised activity–composition models for clinopyroxene and amphibole. Journal of Metamorphic Geology 30, 131–142.

Diener, J.F.A., Powell, R., White, R.W., Holland, T.J.B., 2007. A new thermodynamic model for clino- and orthoamphiboles in the system $Na_2O–CaO–FeO–MgO–Al_2O_3–SiO_2–H_2O–O$. Journal of Metamorphic Geology 25, 631–656.

Dostal, J., Dupuy, C., Caby, R., 1994. Geochemistry of the Neoproterozoic Tilemsi Belt of Iforas (Mali, Sahara)—A Crustal Section of an Oceanic Island-Arc. Precambrian Research 65, 55–69.

Please cite this article as: Doukkari, S.A., et al., Prograde and retrograde evolution of eclogite from Adrar Izzilatène (Egéré-Aleksod terrane, Hoggar, Algeria) determined from chemical..., Lithos (2014), http://dx.doi.org/10.1016/j.lithos.2014.12.007

Dostal, J., Caby, R., Keppie, J.D., Maza, M., 2002. Neoproterozoic magmatism in Southern Algeria in Southern Algeria (Sebkha el Mehla inlier): A northern extension of the Trans Saharian orogenese. Journal of African Earth Sciences 35, 213–225.
Doukkari, S.A., Ouzegane, K., Arab, A., Kienast, J.R., Godard, G., Drareni, A., Zetoutou, S., Liégeois, J.P., 2014. Phase relationships and P–T path in NCFMASHTO system of the eclogite from the Tighsi area (Egere terrane, Central Hoggar, Algeria). Journal of African Earth Sciences 99, 276–286.
Duplan, L., 1972. La chaîne de l'Egéré (Hoggar septentrional). Bulletin du Service géologique de l'Algérie 2 (200 + 157 pp.).
Dziggel, A., Diener, J.F.A., Stoltz, N.B., Kolb, J., 2012. Role of H_2O in the formation of garnet coronas during near-isobaric cooling of mafic granulites: The Tasiusarsuaq terrane, southern West Greenland. Journal of Metamorphic Geology 30, 957–972.
England, P.C., Thompson, A.B., 1984. Pressure-temperature-time paths of regional metamorphism: 1. Heat transfer during the evolution of regions of thickened continental crust. Journal of Petrology 25, 894–928.
Fezaa, N., Liégeois, J.-P., Abdallah, N., Cherfouh, E.H., de Waele, B., Bruguier, O., Ouabadi, A., 2010. Late Ediacaran geological evolution (575–555 Ma) of the Djanet Terrane, Eastern Hoggar, Algeria, evidence for a Murzukian intracontinental episode. Precambrian Research 180, 299–327.
Fitzherbert, J.A., Clarke, G.L., Powell, R., 2005. Preferential retrogression of high-P metasediments and the preservation of blueschist to eclogite facies metabasite during exhumation, Diahot terrane, NE New Caledonia. Lithos 83, 67–96.
Godard, G., 2001. Eclogites and their geodynamic interpretation: A history. Journal of Geodynamics 32, 165–203.
Godard, G., 2009. Two orogenic cycles in eclogite-facies gneisses of the Southern Armorican Massif (France). European Journal of Mineralogy 21, 1173–1190.
Green, E.C.R., Holland, T.J.B., Powell, R., 2007. An order– disorder model for omphacitic pyroxenes in the system jadeite–diopside–hedenbergite–acmite, with applications to eclogitic rocks. American Mineralogist 92, 1181–1189.
Groppo, C., Lombardo, B., Rolfo, F., Pertusati, P., 2007. Clockwise exhumation path of granulitised eclogites from the Ama Drime range (Eastern Himalayas). Journal of Metamorphic Geology 25, 51–75.
Groppo, C., Beltrando, M., Compagnoni, R., 2009. The P–T path of the ultra-high pressure Lago Di Cignana and adjoining high-pressure meta-ophiolitic units: Insights into the evolution of the subducting Tethyan slab. Journal of Metamorphic Geology 27, 207–231.
Guiraud, M., Powell, R., Rebay, G., 2001. H_2O in metamorphism and unexpected behaviour in the preservation of metamorphic mineral assemblages. Journal of Metamorphic Geology 19, 445–454.
Hacker, B.R., Andersen, T.B., Johnston, S., Kylander-Clark, A.R.C., Peterman, E.M., Walsh, E.O., Young, D., 2010. High-temperature deformation during continental-margin subduction and exhumation: The ultrahigh-pressure Western Gneiss region of Norway. Tectonophysics 480, 149–171.
Holland, T.J.B., Powell, R., 1998. An internally consistent thermodynamic data set for phases of petrological interest. Journal of Metamorphic Geology 16, 309–343.
Holland, T.J.B., Powell, R., 2003. Activity–composition relations for phases in petrological calculations: An asymmetric multicomponent formulation. Contributions to Mineralogy and Petrology 145, 492–501.
Koons, P.O., Rubie, D.C., Frueh-Green, G., 1987. The effects of disequilibrium and deformation on the mineralogical evolution of quartz-diorite during metamorphism in the eclogite facies. Journal of Petrology 29, 670–700.
Kretz, R., 1983. Symbols for rock-forming minerals. American Mineralogist 68, 277–279.
Krogh, E.J., 1982. Metamorphic evolution deduced from mineral inclusions and compositional zoning in garnet from Norwegian country- rock eclogites. Lithos 15, 305–321.
Küllerud, K., Flaat, K., Davidsen, B., 2001. High-pressure fluid-rock reactions involving Cl bearing fluids in lower-crustal ductile shear zones of the Flakstadøy basic complex, Lofoten, Norway. Journal of Petrology 42, 1349–1372.
Laird, J., Albee, A.L., 1981. Pressure, temperature, and time indicators in mafic schist—Their application to reconstructing the polymetamorphic history of Vermont. American Journal of Science 281, 127–175.
Lappin, M.A., Smith, D.C., 1978. Mantle-equilibrated orthopyroxene eclogite pods from the basal gneisses in the Selje District, western Norway. Journal of Petrology 19, 530–584.
Latouche, L., 1985. Les collisions intracratoniques et la tectonique tangentielle dans le Pan-Africain du Hoggar central. Evolution géologique de l'Afrique. Publication occasionnelle (CIFEG4, 143le.an).
Leake, B.E., Wooley, A.R., Arps, C.E.S., 1997. Nomenclature of amphiboles, report of the Subcommittee on Amphiboles of the International Mineralogical Association Commission on New Minerals and Mineral Names. European Journal of Mineralogy 9, 623–651.
Lelubre, M., 1952. Recherche sur la géologie de l'Ahaggar central et occidental (Sahara central). Bulletin du Service Géologique de l'Algérie 22 (tome 1, 354 p, tome 2, 387 pp.).
Liégeois, J.P., Stern, R.J., 2010. Sr–Nd isotopes and geochemistry of granite-gneiss complexes from the Meatiq and Hafafit domes, Eastern Desert, Egypt: No evidence for pre-Neoproterozoic crust. Journal of African Earth Sciences 57, 31–40.
Liégeois, J.P., Bertrand, J.M., Black, R., 1987. The subduction-related and collision-related Pan-African composite batholith of the Adrar des Iforas (Mali)—A review. Geological Journal 22, 185–211.
Liégeois, J.P., Latouche, L., Boughrara, M., Navez, J., Guiraud, M., 2003. The LATEA metacraton (Central Hoggar, Tuareg shield, Algeria): Behavior of an old passive margin during the pan-African orogeny. Journal of African Earth Sciences 37, 161–190.
Liégeois, J.P., Benhallou, A., Azzouni-Sekkal, A., Yahiaoui, R., Bonin, B., 2005. The Hoggar swell and volcanism; reactivation of the Precambrian Tuareg Shield during Alpine convergence and West African Cenozoic volcanism. Special Paper - Geological Society of America 388, 379–400.
Liégeois, J.P., Abdelsalam, M.G., Ennih, N., Ouabadi, A., 2013. Metacraton: Nature, genesis and behavior. Gondwana Research 23, 220–237.
Maupin, V., Agostini, A., Artemieva, I., Balling, N., Beekman, F., Ebbing, J., England, R.W., Frassetto, A., Gradmann, S., Jacobsen, B.H., Köhler, A., Kvarven, T., Medhus, A.B., Mjelde, R., Ritter, J., Sokoutis, D., Stratford, W., Thybo, H., Wawerzinek, B., Weidle, C., 2013. The deep structure of the Scandes and its relation to tectonic history and present-day topography. Tectonophysics 602, 15–37.
Morimoto, N., 1988. Nomenclature of pyroxenes. Mineralogical Magazine 52, 535–550.
Nouar, O., Henry, B., Liégeois, J.P., Derder, M.E.M., Bayou, B., Bruguier, O., Ouabadi, A., Amenna, M., Hemmi, A., Ayache, M., 2011. Eburnean and Pan-African granitoids and the Raghane mega-shear zone evolution: Image analysis, U–Pb zircon age and AMS study in the Arokam Ténéré (Tuareg shield, Algeria). Journal of African Earth Sciences 60, 133–152.
Ouzegane, K., Kienast, J.R., Bendaoud, A., Drareni, A., 2003. A review of Archaean and Paleoproterozoic evolution of the In Ouzzal granulitic terrane (Western Hoggar, Algeria). Journal of African Earth Sciences 37, 207–227.
Peucat, J.J., Drareni, A., Latouche, L., Deloule, E., Vidal, P., 2003. U-Pb zircon (TIMS and SIMS) and Sm-Nd whole rock geochronology of the Gour Oumelalen granulitic basement Hoggar massif, Tuareg shield, Algeria. Journal of African Earth Sciences 37, 229–239.
Powell, R., 1978. Equilibrium Thermodynamics in Petrology. Harper and Row, London (284 pp.).
Powell, R., Holland, T.J.B., 1988. An internally consistent thermodynamic dataset with uncertainties and correlations: 3. Applications to geobarometry, worked examples and a computer program. Journal of Metamorphic Geology 6, 173–204.
Rebay, G., Powell, R., Diener, J.F.A., 2010. Calculated phase equilibria for a MORB composition in a P–T range, 450–650 °C and 18–28 kbar: The stability of eclogite. Journal of Metamorphic Geology 28, 635–645.
Rougier, S., Missenard, Y., Gautheron, C., Barbarand, J., Zeyen, H., Pinna, R., Liégeois, J.P., Bonin, B., Ouabadi, A., Derder, M.E.M., Frizon de Lamotte, D., 2013. Eocene exhumation of the Tuareg Shield (Sahara, Africa). Geology 41, 615–618.
Sautter, V., 1985. An eclogite paragenesis from the Aleksod basement, Central Hoggar, South Algeria. Chemical Geology 50, 331–347.
Sautter, V., 1986. Les éclogites de 1'Aleksod (sud algérien): Des témoins in situ d'une collision intracontinentale. Journal of African Earth Sciences 5, 345–357.
Stern, R.J., 2002. Subduction Zones.
Štĭpskà, P., Powell, R., 2005. Constraining the P–T path of a MORB-type eclogite using pseudosections, garnet zoning and garnet-clinopyroxene thermometry: An example from the Bohemian Massif. Journal of Metamorphic Geology 23, 725–743.
White, R.W., Powell, R., Holland, T.J.B., Worley, B.A., 2000. The effect of TiO_2 and Fe_2O_3 on metapelitic assemblages at greenschist and amphibolite facies conditions: Mineral equilibria calculations in the system K_2O-FeO-MgO-Al_2O_3-SiO_2-H_2O-TiO_2-Fe_2O_3. Journal of Metamorphic Geology 18, 497–511.
White, R.W., Powell, R., Holland, T.J.B., 2007. Progress relating to calculation of partial melting equilibria for metapelites. Journal of Metamorphic Geology 25, 511–527.
Zetoutou, S., Ouzegane, K., Boubazine, S., Kienast, J.R., 2004. Azrou N' Fad (Central Hoggar, Algeria) one of the deepest terranes of LATEA: Arguments based on P–T evolution in eclogites. Journal of African Earth Sciences 39, 193–200.
Zhang, R.Y., Liou, J.G., 1997. Partial transformation of gabbro to coesite-bearing eclogite from Yangkou, the Sulu terrane, eastern China. Journal of Metamorphic Geology 15, 183–202.
Zhang, R.Y., Liou, J.G., 1997. Partial transformation of gabbro to coesite-bearing eclogite from Yangkou, the Sulu terrane, eastern China. Journal of Metamorphic Geology 15, 183–202.
Zheng, Y.F., Fu, B., Gong, B., Li, L., 2003. Stable isotope geochemistry of ultrahigh pressure metamorphic rocks from the Dabie-Sulu orogen in China: Implications for geodynamics and fluid regime. Earth-Science Reviews 62, 105–161.

Please cite this article as: Doukkari, S.A., et al., Prograde and retrograde evolution of eclogite from Adrar Izzilatène (Egéré-Aleksod terrane, Hoggar, Algeria) determined from chemical..., Lithos (2014), http://dx.doi.org/10.1016/j.lithos.2014.12.007